to S. Terai for secretarial assistance. This work was supported in part by grants-in-aid for Scientific Research from the Ministry of Education, Science and Culture of Japan, the Yamanouchi Foundation for Research on Metabolic Disorders, the Mochida Memorial Foundation for Medical and Pharmaceutical Research, and the Takeda Science Foundation.

REFERENCES

1. Hardy, M. H. (1992) *Trends Genet.* **8,** 55–61.
2. Dry, F. W. (1926) *J. Genet.* **16,** 287–340.
3. Chase, H. B. (1954) *Physiol. Rev.* **34,** 113–126.
4. Paus, R., Foitzik, K., Welker, P., Bulfone-Paus, S., and Eichmüller, S. (1997) *J. Invest. Dermatol.* **109,** 518–526.
5. Hebert, J. M., Rosenquist, T., Gotz, J., and Martin, G. R. (1994) *Cell* **78,** 1017–1025.
6. Müller-Röver, S., Bulfone-Paus, S., Handjiski, B., Welker, P., and Sundberg, J. P., McKay, I. A., Botchkarev, V. A., and Paus, R. (2000) *J. Histochem. Cytochem.* **48,** 557–568.
7. Tosti, A., Misciali, C., Piraccini, B. M., Peluso, A. M., and Bardazzi, F. (1994) *Drug Saf.* **10,** 310–317.
8. Pillans, P. I., and Wood, D. J. (1995) *Int. J. Dermatol.* **34,** 149–158
9. Hanson, W. R., Pelka, A. E., Nelson, A. K., and Malkinson, F. D. (1992) *Int. J. Radiat. Oncol. Biol. Phys.* **23,** 333–337.
10. Michelet, J. F., Commo, S., Billoni, N., Mahe, Y. F., and Bernard, B. A. A. (1997) *J. Invest. Dermatol.* **108,** 205–209.
11. Goldyne M. E. (1975) *J. Invest. Dermatol.* **64,** 377–385.
12. Fürstenberger, G., and Marks, F. (1980) *Biochem. Biophys. Res. Commun.* **92,** 749–756.
13. Pentland, A. P., and Needleman, P. (1986) *J. Clin. Invest.* **77,** 246–251.
14. Zhang, J. Z., Maruyama, K., Iwatsuki, K., Ono, I., and Kaneko, F. (1994) *Exp. Dermatol.* **3,** 164–170.
15. Scholz, K., Furstenberger, G., Müller-Decker, K., and Marks, F. (1995) *Biochem. J.* **309,** 263–269.
16. Langenbach, R., Loftin, C., Lee, C., and Tiano, H. (1999) *Biochem. Pharmcol.* **58,** 1237–1246.
17. Müller-Decker, K., Scholz, K., Neufang, G., Marks, F., and Furstenberger, G. (1998) *Exp. Cell. Res.* **242,** 84–91.
18. Negishi, M., Sugimoto, Y., and Ichikawa, A. (1995) *Biochim. Biophys. Acta* **1259,** 109–119.
19. Narumiya, S., Sugimoto, Y., and Ushikubi, F. (1999) *Physiol. Rev.* **79,** 1193–1226.
20. Suzuki, S., Ota, Y., Ozawa, K., and Imamura, T. (2000) *J. Invest. Dermatol.* **114,** 456–463.
21. Sugimoto, Y., Namba, T., Shigemoto, R., Ichikawa, A., and Narumiya, S. (1994) *Am. J. Physiol.* **266,** F823–F828.
22. Watanabe, T., Nakao, A., Emerling, D., Hashimoto, Y., Tsukamoto, K., Horie, Y., Kinoshita, M., and Kurokawa, K. (1994) *J. Biol. Chem.* **269,** 17619–17625.
23. Arakawa, T., Laneuville, O., Miller, C. A., Lakkides, K. M., Wingerd, B. A., Dewitt, D. L., and Smith, W. L. (1996) *J. Biol. Chem.* **271,** 29569–29575.
24. Paus, R., and Cotsarelis, G. (1999) *N. Engl. J. Med.* **341,** 491–497.
25. Dubravsky, N. B., Hunter, N., Mason, K., and Withers, H. R. (1978) *Radiology* **126,** 799–802.
26. Stenn, K. S., and Paus, R. (2001) *Physiol. Rev.* **81,** 449–494.
27. Neufang, G., Fürstenberg, G., Heidt, M., Marks, F., and Müller-Decker K. (2001) *Proc. Natl. Acad. Sci. USA* **98,** 7629–7634.

Biochemical and Biophysical Research Communications 292, 675–681 (2002)
doi:10.1006/bbrc.2002.6698, available online at http://www.idealibrary.com on IDEAL®

Apoptosis and Related Proteins during Parturition in Prostaglandin F Receptor-Deficient Mice[1]

Junwu Mu,*[,2] Toru Kanzaki,* Xiaoe Si,† Takuji Tomimatsu,* Hirotsugu Fukuda,* Eriko Fujii,* Takayoshi Hosono,* Yuji Murata,* Yukihiko Sugimoto,‡ and Atsushi Ichikawa‡

**Department of Obstetrics and Gynecology and †Radiation Biology, Osaka University, Faculty of Medicine, 2-2 Yamadaoka Suita, Osaka 565-0871, Japan; and ‡Department of Physiological Chemistry, Faculty of Pharmaceutical Sciences, Kyoto University, Sakyo-ku, Kyoto 606-8501, Japan*

Received February 25, 2002

This study investigated whether apoptosis and related proteins are involved in parturition by comparative observation of FP-deficient mice without labor and wild type mice with vaginal delivery. We examined the expression of apoptosis, Fas, FasL, active caspase-3 and bcl-2 proteins in the amnion, placenta and decidua. DNA laddering in the amnion, placenta and decidua tissue did not significantly differ between FP-deficient and wild type mice on day 18 of pregnancy. Similar TUNEL staining results were found in all tissues of FP-deficient mice compared with those of wild type mice. A higher intensity of apoptotic cells was found in the decidua basalis. The index of TUNEL-positive cells were not significantly different in the amnion, placenta and decidua of FP-deficient mice compared with that of wild type mice on day 18 of pregnancy. Specific bands for Fas were clearly observed in the amnion, placenta and decidua tissue. FasL specific bands were observed in the placenta and decidua, but a few in amnion tissue. A great number of active caspase-3 specific bands were detected in decidua, while a few such bands were detected in the placenta and few bands in the amniotic tissue. Bands for bcl-2 were detected in the amnion, placenta and decidua tissue. The weakest band was in decidual tissue. Fas, FasL, active caspase-3, and bcl-2 specific bands did not show any significant differences between the two groups. These findings demonstrate that apoptosis, Fas, FasL, caspase-3, and Bcl-2 occur in mouse term placenta that is not involved in parturition. © 2002 Elsevier Science (USA)

Key Words: **apoptosis; Fas; FasL; caspase; Bcl-2; parturition; placenta; mouse.**

Apoptosis is a form of programmed cell death that is controlled at the gene level, and it plays important roles in embryonic development, in the maintenance of tissue homeostasis, and in the elimination of cells that have suffered serious DNA damage (1, 2). Apoptosis has recently been implicated in regulating various reproductive tissues, including those of the uterus (3) ovary (4) placenta (5) fetal membranes (6). In humans, apoptosis has been described in placentas from normal pregnancies and is reported to be increased in pregnancies complicated by fetal growth restriction (7, 8). Increased incidence of apoptosis has been demonstrated in syncytiotrophoblast of failing first trimester pregnancies (9, 10).

Apoptosis is specifically induced via signaling through a family of receptors known collectively as 'death receptors' including Fas, TNFR, DR3, -4, and -5. Fas is a type I membrane protein that belongs to the tumor necrosis factor and nerve growth factor family (11). FasL is a type II membrane protein also related to the tumor necrosis factor family. FasL binding induces Fas trimerization and recruits initiator caspase-8 and 10 via the adaptor protein FADD (Fas-associated death domain). Caspase-8 then cleaves and activates caspase-3. Caspase 3 is one of the key executioners and is essential and specific for apoptosis (12, 13). When it is activated, it is cleaved into a small prodomain and two submits of 17 and 12 kDa, and cleaves endogenous substrate protein, finally causing the degradation of chromosomal DNA into nucleosomal units characteristic of apoptosis (14). Bcl-2 was first discovered in human follicular lymphoma and was regarded as a proto-oncogene (15). It was reported that Bcl-2 has the function of inhibiting apoptosis (16, 17).

Prostaglandin $F_{2\alpha}$ is believed to play an important role in the regulation of myometrial contractility and initiation of parturition. The receptors for prostaglandin $F_{2\alpha}$ (FP)-deficient mice are unable to induce a spon-

[1] This work is partly supported by Grant 13671711 from the Ministry of Education, Culture, Sports, Science and Technology, Japan.

[2] To whom correspondence and reprint requests should be addressed. Fax: +81-6-6879-3359. E-mail: mujunwu@hotmail.com.

0006-291X/02 $35.00

taneous labor even 1 week after term due to a failure of the corpora lutea to cease progesterone production (18). In humans, whether apoptosis in the placenta is associated with labor remains controversial. Mice lacking the prostaglandin F receptor provide an animal model with normal gestation but failure to initiate labor and delivery at term, continuing the pregnancy instead. This study investigated whether apoptosis and its related proteins are involved in parturition by a comparative observation of wild type mice with vaginal delivery and FP-deficient mice without labor.

MATERIALS AND METHODS

All animals were maintained in accordance with institutional guidelines for care and use of laboratory animals. Mice were housed under standard lighting (12 h light:12 h darkness) and temperature (23 ± 1°C). Mice were also given free access to a nutritionally balanced diet and tap water.

Prostaglandin $F_{2\alpha}$ (FP) receptor-deficient mice were obtained as described previously (18). Normal adult female mice with the ± genotype bred in our animal facility were mated with either FP-deficient male mice or male mice with the ± genotype, and the resulting female FP-deficient mice and wild type mice were used in the present experiment. The mouse genotypes were identified by polymerase chain reaction.

The day a copulation plug was found was considered day 0 of pregnancy. Wild type mice delivered normal fetuses at term (day 18 or 19), but FP-deficient mice were unable to deliver fetuses. Amnions, placentas and deciduas were removed from fetuses on day 18 of pregnancy. At the same time, the number of pups, survival, and weight were recorded. Half of placentas from the same mice were fixed in a 10% formaldehyde neutral buffer solution and embedded in paraffin. Five sections were cut for each sample. The other placentas were isolated by gently separating amnion, placenta and deciduas tissues. All tissues were flash frozen, and stored at −80°C until processed for DNA fragmentation assay and Western blot analysis.

DNA fragmentation assay. The amniotic, placental and decidual tissues dissected were immediately frozen in liquid nitrogen. Each sample was homogenized in 300 to 500 μl of lysis buffer (100 mM Tris–HCl, pH 8.5, 5 mM EDTA, 200 mM NaCl, 0.2% SDS, pH 8.0, 0.5% Triton X-100) and 10 μl proteinase K (10 mg/ml) followed by overnight incubation at 37°C. The samples were then incubated with 5 μl of RNase A (10 mg/ml) for 30 min at 37°C, and DNA was extracted with isopropanol. DNA was precipitated with 70% ethanol, air dried, suspended in a TE buffer, incubated at 37°C for 60 min, and left overnight at 4°C DNA (15 μg from each sample) was electrophoretically separated on a 1.8% agarose gel. The gel was stained with 0.02% ethidium bromide to visualize the DNA fragmentation and photographed.

In situ detection of DNA nicking. Detection of fragmentation was performed using the terminal deoxynucleotidyl transferase-mediated dUDP nick end-labeling (TUNEL) technique. Briefly, consecutive sections (5-μm) from formalin-fixed, paraffin-embedded tissue blocks were placed on coated slides for use in a molecular biological–histochemical system. The TUNEL procedure was performed using an Apop Tag kit (Oncor, Gaithersburg, MD) according to the manufacturer's instructions. The tissue sections were deparaffinized and protein was digested with 20 μg/ml proteinase K for 15 min at room temperature. Endogenous peroxidase activity was quenched with 3% H_2O_2 in phosphate-buffered saline. After washing with PBS, an equilibration buffer was applied directly to the specimen. Terminal deoxynucleotidyl transferase (TdT) enzyme and dUTP-dioxigenin were added and incubated at 37°C for 1 h in a humidified chamber. The reaction was then stopped with a stop/wash buffer supplied with the kit, and the slides were incubated with an anti-digoxigenin-peroxidase solution for 30 min at room temperature, colorized with DAB/H_2O_2, and counterstained with methyl green. Negative controls were processed with labeled dUTP in the absence of the TdT enzyme. Sections of normal rodent mammary gland were used as positive controls. The apoptotic index was obtained by dividing the number of apoptotic cells by the total number of cells counted and multiplying the result by 100.

TABLE 1

Characteristics of FP-Deficient and Wild Type Pregnant Mice

	Wild type	FP-deficient	Statistics
Maternal mouse (week)	14 ± 3.2	14 ± 3.5	NS
Parity	0	0	NS
Day of pregnancy	18	18	NS
Body weight of fetus (g)	1.18 ± 0.12	1.19 ± 0.11	NS
Number of fetus	8.3 ± 1.7	7.5 ± 1.5	NS

Note. All values were expressed as means ± SD. NS, nonsignificant.

Western blot analysis. Each sample was homogenized in a lysis buffer (0.01 M Tris, pH 7.8, 0.1 M NaCl, 0.1 mM EDTA, 1 mM PMSF, pepstatin 2 μg/ml, leupeptin, and chymostatin 2 μg/ml) and centrifuged at 12,000*g* for 10 min at 4°C and the supernatants were stored at −80°C. Then, the protein concentration of the lysates was determined with a BCA protein assay kit (Pierce, Rockford, IL), samples (50 μg) were denatured in a gel loading buffer at 100°C for 3 min and loaded on a 15% SDS–polyacrylamide gel. After electrophoresis, proteins were transferred to nitrocellulose membranes. Blocking was performed with PBST (phosphate-buffered saline containing 0.1% Tween 20), containing 5% nonfat dried milk solution for 1 h. The transferred membrane was incubated with the primary antibody for Fas, FasL, and Bcl-2 (polyclonal Ab M-20, N-20 and N-19 at 1:1000 dilution; Santa Cruz Biotechnology Inc.); for caspase-3 (polyclonal Ab D-175 at 1:1000 dilution; Cell Signaling) for 24 h at 4°C. After washing, horseradish-peroxidase-conjugated anti-rabbit immunoglobulin G (IgG) was applied at a 1:1000 dilution for 1 h at room temperature. The blot was washed in PBS-T three times and visualized with an enhanced chemiluminescence (ECL) Western blotting detection system (Amersham).

Statistical analysis. Values were expressed as means and standard deviations. Statistical analysis between the groups was performed by using Student's t test and Mann–Whitney U test. Values were considered statistically significant at $P < 0.05$.

RESULTS

There were no significant differences in maternal age, parity, day of pregnancy, weight of fetus and number of fetuses between FP-deficient mice without labor and wild type mice with normal delivery (Table 1). There are no differences in the weights of placenta and decidua on day 18 of pregnancy between the two groups in a previous report (19).

DNA Fragmentation Assay

To determine whether apoptosis occurred in the mouse amnion, placenta and decidua, DNA fragmentation assay was performed using these tissues. DNA

fragments from the amnion, placental and decidual tissue can be detected by the "DNA ladder" on agarose gel electrophoresis (Fig. 1). DNA fragmentation was always more pronounced in decidual tissue than amnion and placenta. DNA laddering was not significantly different between FP-deficient and wild type mice at day 18 of pregnancy in the amniotic, placental and decidual tissue.

In Situ Detection of DNA Nicking

Apoptosis has also been demonstrated by the TUNEL method in various cell types within amniotic, placental and decidual tissues. Similar TUNEL staining results were found in amnion, placenta and decidua of FP-deficient mice compare with those of wild type mice (Fig. 2). In amnion, apoptosis was observed in scattered areas in amnion epithelial cells, and beneath the basal lamina of the amnion (Figs. 2A and 2D). The distribution of apoptosis in the amnion was presented in clusters. In the placenta, most TUNEL-positive cells were found in trophoblast and stromal cells (Figs. 2B and 2E). A higher intensity of apoptotic cells was found in the decidual basalis (Figs. 2C and 2F); however, these apoptotic cells were not uniformly distributed. The main area demonstrating these cells was the center of the decidual basalis, and the intensity decreased toward the placental margin. The index of TUNEL-positive cells did not significantly differ in the amnion, placenta and decidua of FP-deficient mice compared with that of wild type mice on day 18 of pregnancy (Fig. 3).

Western Blot Analysis

We examined the expression of Fas, FasL, active caspase-3 and bcl-2 proteins in the amnion, placenta and decidua by western blotting analysis. Figure 4 revealed a major band of approximately 45 kDa for Fas, 40 kDa for FasL, 17 kDa for active caspase-3 and 26 kDa for Bcl-2 running at the same molecular mass. Specific bands for Fas were clearly observed in the amnion, placenta and decidua tissue. FasL specific bands were clearly observed in placenta and weakly in decidua, but few in amniotic tissue. There were no significant differences in Fas and FasL between FP-deficient and wild type mice. There were a greater number of active caspase-3 specific bands were more detected in decidua and a few in the placenta, few in amniotic tissue. Bands for bcl-2 were detected clearly in amniotic, placental and decidual tissue. The weakest band was detected in decidual tissues. Neither the active caspase-3 nor bcl-2 specific bands demonstrated significant differences between FP-deficient mice without labor and wild type mice with vaginal delivery.

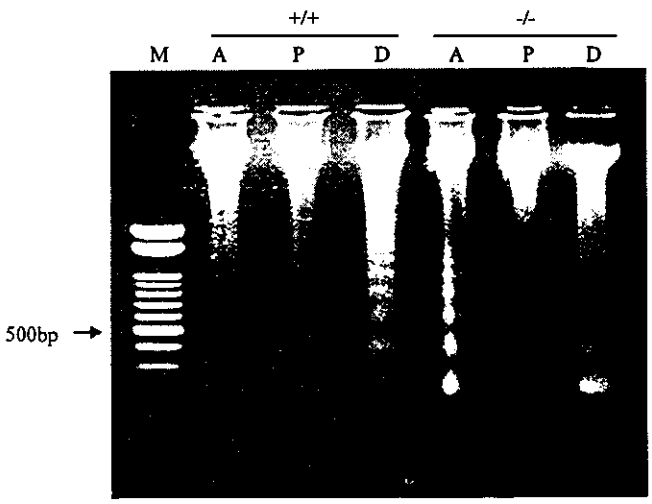

FIG. 1. Electrophoretic analysis of DNA fragmentation in amniotic, placental, and decidual tissue at day 18 of pregnancy between wild type mice with normal delivery and FP-deficient mice without labor. Equal amounts DNA (15 μl) were electrophoretically separated on 1.8% agarose gels and stained with ethidium bromide. A 100-bp DNA ladder was used to reference the molecular size. +/+, wild type; −/−, FP-deficient mice; A, amnion; P, placenta; D, decidua; M, molecular marker.

DISCUSSION

The mechanism by which human and mouse labor is initiated remains largely unknown. It is believed that initiation of labor may involve a maternal–fetal communication process. It has been suggested that the metabolic functions of the human amnion might contribute to the initiation of parturition (20). The incidence of apoptosis in human and mouse placental tissue was reported to progressively increase throughout pregnancy and until close to delivery (7, 19, 21). However, whether apoptotic machinery was associated with parturition at term remains to be elucidated.

In the present study, we demonstrated a similar degree of apoptosis in amnion, placenta and decidua between FP-deficient mice without labor and wild type mice with normal delivery by the TUNEL method and DNA fragmentation assay. As reported previously, female FP-deficient mice do not deliver fetuses at term, although these can be successfully rescued by cesarean section (18). No parturition occurred irrespective of the genotypes of the mating males. There were no abnormalities observed in the weights of placentas and deciduas or histology of the placentas from FP-deficient mice compared with those from wild type mice, although induction of labor is lacking in FP-deficient mice. Lei *et al.* reported that the rat amnion epithelial cells underwent apoptosis before the onset of active labor (22). Hsu *et al.* provided further evidence that a significantly higher apoptosis in amnion epithelial cells of patients with term labor than in those of pa-

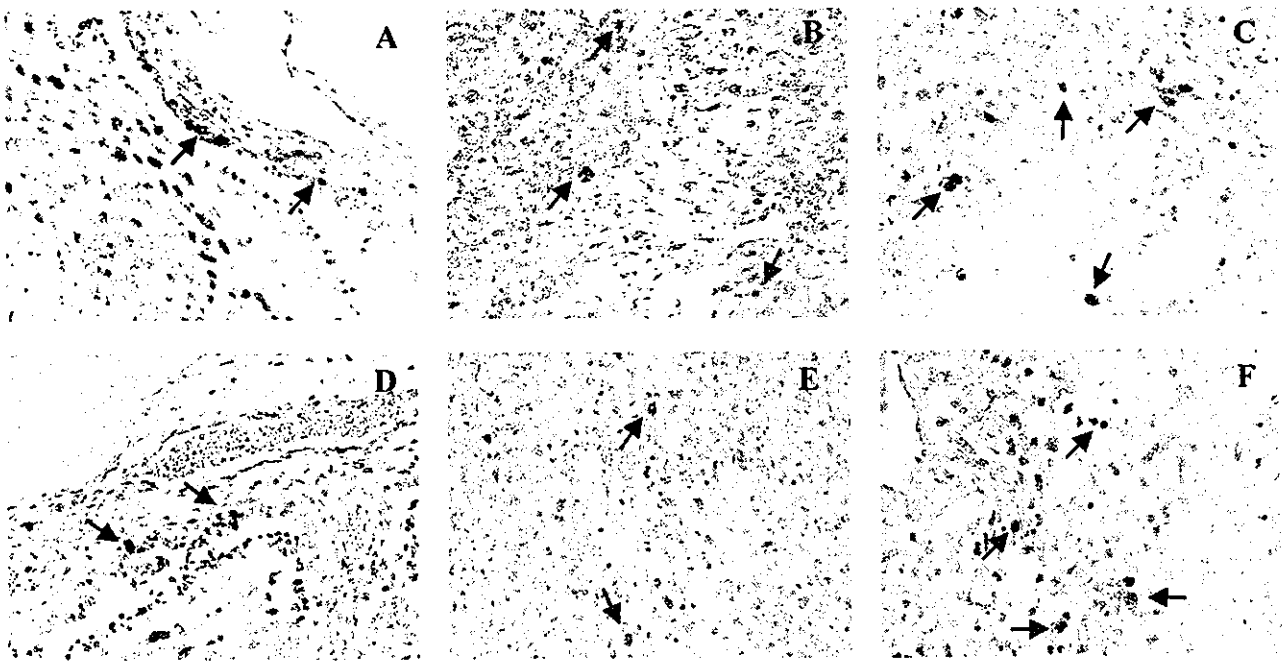

FIG. 2. TUNEL staining in amnion, placenta and decidua from wild type (A, B, C) and FP-deficient mice (D, E, F) at day 18 of pregnancy. Dark-brown staining indicates a positive reaction (arrows). Tissues were counterstained with 1% methyl green. Original magnification, ×200.

tients undergoing elective C/S without labor (23). These observations suggest that apoptosis in amnion epithelial cells can be strongly associated with labor at term in the rat and human. However, a similar incidence of apoptotic nuclei was similar in placentae obtained before the initiation of labor and after delivery has been described (8, 24). Runic and co-workers also demonstrated that apoptosis occurs as part of a program of senescence in chorionic and decidual cells that are not triggered in association with labor (6). Our results further confirm previous observations reporting apoptosis might be involved in a mechanism of placental senescence that is not related to parturition in human placenta (8, 16, 24).

In the present study we have demonstrated expression of Fas in amnion, placenta and decidua tissue and FasL in placenta and decidua, but few in amniotic tissue. The major function of Fas/FasL interaction and Fas activation is the induction of cell apoptosis (11, 25). Fas/FasL-mediated apoptosis is a process that is important not only for normal placentation but also for the establishment of the fetal allograft (26–28). We detected enhanced bands for Fas and FasL in placenta. Huppertz *et al.* localized the expression of FasL to the villous cytotrophoblast in first trimester placentae, whereas the Fas receptor localized to the microvillous surface of syncytiotrophoblast (29). Other authors identified FasL in both layers of the trophoblast throughout gestation (6, 30, 31). In the villous part of the placenta, where FasL is mainly present on cells that have no contact with maternal tissue or blood, the Fas/FasL system is more probably involved in placenta growth. In contrast, in the decidua the presence of FasL on extravillous trophoblast cells may play an important role in the maintenance of immune privilege in the pregnant uterus, by endowing fetal trophoblast cells with a defense mechanism against activated maternal leukocytes. The reduced Fas expression and function in term cytotrophoblasts associated with parturition in humans (32). However, there were no significant differences in Fas and FasL on amnion, placenta and decidua tissue between FP-deficient and wild type mice in our study. Similar to our results, there was no association of Fas or FasL with the pres-

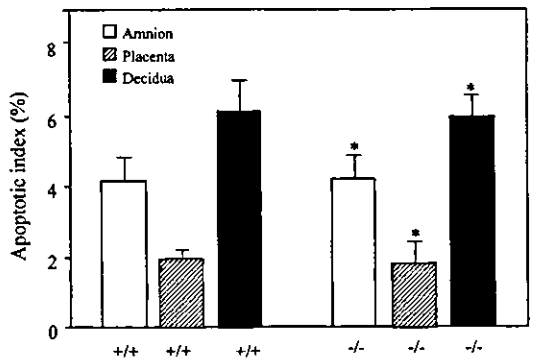

FIG. 3. Comparison of incidences of apoptosis in amnion, placenta, and decidua from wild type (+/+) and FP-deficient mice (−/−) at day 18 of pregnancy. The data represented the mean and SD of 10 to 12 samples from different fetuses. *$P > 0.05$, compared with wild type mice.

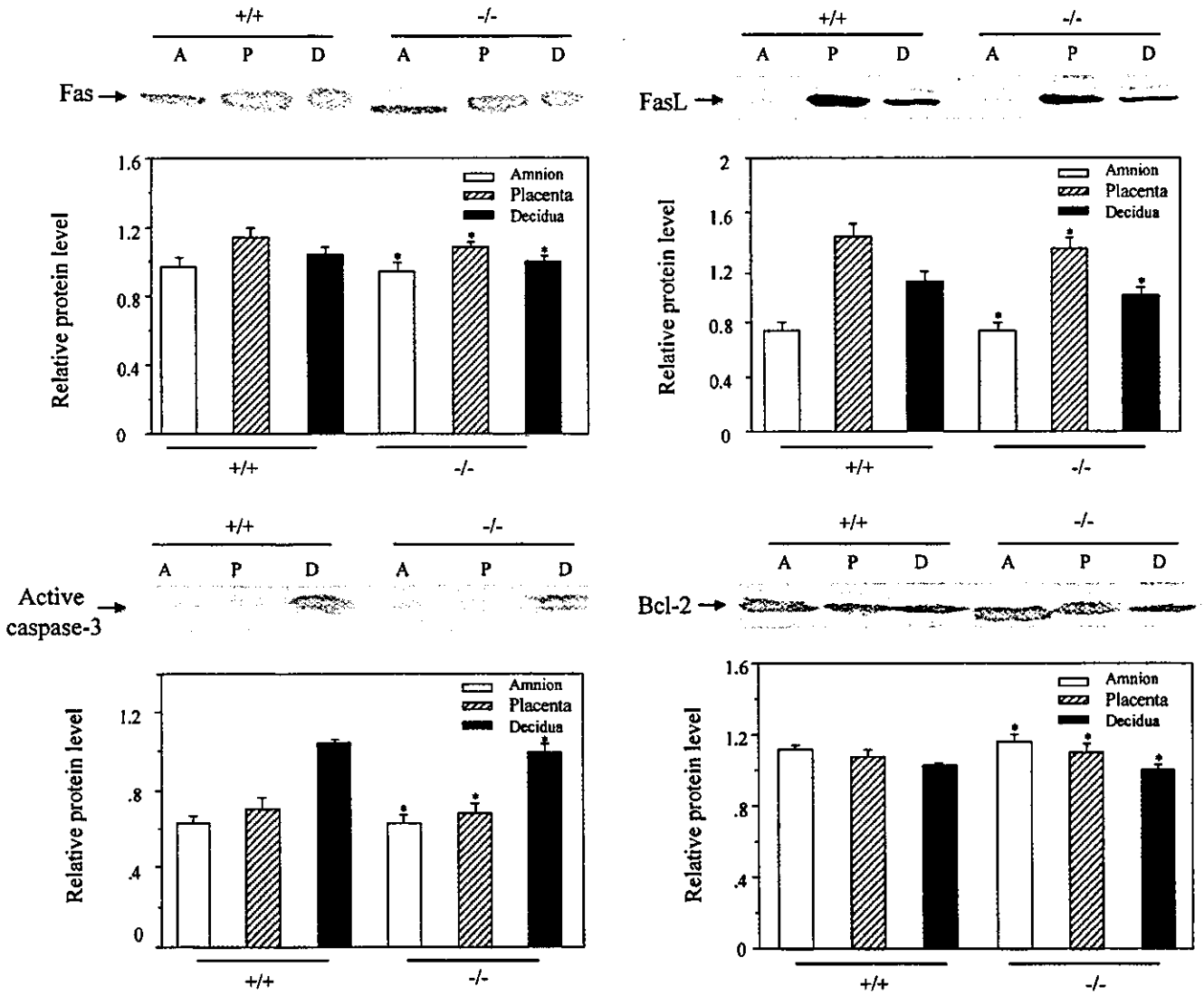

FIG. 4. Western blot analysis of the expression of Fas, FasL, active caspase-3, and bcl-2 in amnion, placenta, and decidua from wild type (+/+) and FP-deficient mice (−/−) at day 18 of pregnancy. The upper panel was a representative experiment; the lower panel was summary of the densitometric analysis from three to four independent experiments for each protein. Relative protein levels in decidual tissue of FP-deficient mice were given a value of 1. Values were the mean and SD. *$P > 0.05$, compared with wild type mice. A, amnion; P, placenta; D, decidua.

ence or absence of labor in human amnion in a study by Kumagai *et al.* (33). It is thought that Fas/FasL may contribute to protecting of the semi-allogeneic fetus from rejection, but is not associated with labor (28, 33, 34).

The induction of apoptosis by most agents in mammalian cells has been found to be caspase-dependent (35). Most studies of caspase were performed in the ischemic brain (36–38), but the role of the caspase in the regulation of programmed cell death in the placenta has not been well studied. In the present study, there were a greater number of active caspase-3 specific bands detected in decidua and a few in the placenta, but few in amniotic tissue at term. This is consistent with the greater degree of apoptosis in the decidua. Higher levels of caspase-3 are expressed in cytotrophoblasts and syncytiotrophoblasts in the first compared to third trimester villi (29). However, active caspase-3 increased in human fetal membrane at term (33). Whether caspase-3-independent pathway also regulates the placental apoptosis is not yet known. In this study, there were no significant differences in active caspase-3 between FP-deficient and wild type mice.

We also identified bcl-2 expression in all tissues examined in mouse term pregnancy. The lower bcl-2 expression in decidual tissue might be related to the induction of apoptosis by increasing the expression of

active caspase-3. Caspase activity is regulated by the bcl-2 family of proteins (39–42). Lea *et al.* examined the immunostaining of bcl-2, a proto-oncogene believed to inhibit apoptosis, from failing in the first trimester pregnancies. Immunostaining of bcl-2 was less intense in failing pregnancies (43). Kim *et al.* reported that the degree of bcl-2 expression significantly decreased in placenta after a gestational period of 32 weeks, and this may be a parturition-associated biological change for inducing apoptosis in the placental villi (44). Bcl-2 protein expression also participates in the regulation of extravillous trophoblast apoptosis (45). Further, an inverse relationship has been identified between apoptosis and bcl-2 expression in syncytiotrophoblasts (46). There was no significant difference in bcl-2 between the subjects that underwent labor and those that did not, and between the vaginal delivery group and the caesarean section group (33). Bcl-2 expression might be an important factor in the regulation of apoptosis in placenta and thus in maintaining placental function during gestation, but not in the induction of labor.

In conclusion, it seems likely that Fas, FasL, caspase-3, and Bcl-2 expressions participate in the regulation of amniotic, placental and decidual apoptosis during pregnancy in mice. Similar expressions of apoptosis and related proteins were found at term pregnancy in FP-deficient and wild type mice, suggesting that these proteins are not involved in parturition.

REFERENCES

1. Kerr, J. F., Winterford, C. M., and Harmon, B. V. (1994) Apoptosis. Its significance in cancer and cancer therapy. *Cancer* **73,** 2013–2026.
2. Hale, A. J., Smith, C. A., Sutherland, L. C., Stoneman, V. E., Longthorne, V. L., Culhane, A. C., and Williams, G. T. (1996) Apoptosis: Molecular regulation of cell death. *Eur. J. Biochem.* **236,** 1–26.
3. Watanabe, H., Kanzaki, H., Narukawa, S., Inoue, T., Katsuragawa, H., Kaneko, Y., and Mori, T. (1997) Bcl-2 and Fas expression in eutopic and ectopic human endometrium during the menstrual cycle in relation to endometrial cell apoptosis. *Am. J. Obstet. Gynecol.* **176,** 360–368.
4. Hsueh, A. J., Billig, H., and Tsafriri, A. (1994) Ovarian follicle atresia: A hormonally controlled apoptotic process. *Endocr. Rev.* **15,** 707–724.
5. Smith, S. C., Baker, P. N., and Symonds, E. M. (1997) Placental apoptosis in normal human pregnancy. *Am. J. Obstet. Gynecol.* **177,** 57–65.
6. Runic, R., Lockwood, C. J., LaChapelle, L., Dipasquale, B., Demopoulos, R. I., Kumar, A., and Guller, S. (1998) Apoptosis and Fas expression in human fetal membranes. *J. Clin. Endocrinol. Metab.* **83,** 660–666.
7. Smith, S. C., Baker, P. N., and Symonds, E. M. (1997) Increased placental apoptosis in intrauterine growth restriction. *Am. J. Obstet. Gynecol.* **177,** 1395–1401.
8. Axt, R., Kordina, A. C., Meyberg, R., Reitnauer, K., Mink, D., and Schmidt, W. (1999) Immunohistochemical evaluation of apoptosis in placentae from normal and intrauterine growth-restricted pregnancies. *Clin. Exp. Obstet. Gynecol.* **26,** 195–198.
9. Kokawa, K., Shikone, T., and Nakano, R. (1998) Apoptosis in human chorionic villi and decidua in normal and ectopic pregnancy. *Mol. Hum. Reprod.* **4,** 87–91.
10. Qiao, S., Nagasaka, T., Harada, T., and Nakashima, N. (1998) p53, Bax and Bcl-2 expression, and apoptosis in gestational trophoblast of complete hydatidiform mole. *Placenta* **19,** 361–369.
11. Nagata, S., and Golstein, P. (1995) The Fas death factor. *Science* **267,** 1449–1456.
12. Armstrong, R. C., Aja, T. J., Hoang, K. D., Gaur, S., Bai, X., Alnemri, E. S., Litwack, G., Karanewsky, D. S., Fritz, L. C., and Tomaselli, K. J. (1997) Activation of the CED3/ICE-related protease CPP32 in cerebellar granule neurons undergoing apoptosis but not necrosis. *J. Neurosci.* **17,** 553–562.
13. Srinivasan, A., Roth, K. A., Sayers, R. O., Shindler, K. S., Wong, A. M., Fritz, L. C., and Tomaselli, K. J. (1998) In situ immunodetection of activated caspase-3 in apoptotic neurons in the developing nervous system. *Cell Death Differ.* **5,** 1004–1016.
14. Enari, M., Sakahira, H., Yokoyama, H., Okawa, K., Iwamatsu, A., and Nagata, S. (1998) A caspase-activated DNase that degrades DNA during apoptosis, and its inhibitor ICAD. *Nature* **391,** 43–50.
15. Tsujimoto, Y., Cossman, J., Jaffe, E., and Croce, C. M. (1985) Involvement of the bcl-2 gene in human follicular lymphoma. *Science* **228,** 1440–1443.
16. Vaux, D. L., Cory, S., and Adams, J. M. (1988) Bcl-2 gene promotes haemopoietic cell survival and cooperates with c-myc to immortalize pre-B cells. *Nature* **335,** 440–442.
17. Kroemer, G. (1997) The proto-oncogene Bcl-2 and its role in regulating apoptosis. *Nat. Med.* **3,** 614–620.
18. Sugimoto, Y., Yamasaki, A., Segi, E., Tsuboi, K., Aze, Y., Nishimura, T., Oida, H., Yoshida, N., Tanaka, T., Katsuyama, M., Hasumoto, K., Murata, T., Hirata, M., Ushikubi, F., Negishi, M., Ichikawa, A., and Narumiya, S. (1997) Failure of parturition in mice lacking the prostaglandin F receptor. *Science* **277,** 681–683.
19. Mu, J., Kanzaki, T., Tomimatsu, T., Fukuda, H., Wasada, K., Fujii, E., Endoh, M., Kozuki, Y., Murata, Y., Sugimoyo, Y., and Ichikawa, A. (2002) Expression of apoptosis in placentas from mice lacking the prostaglandin F receptor. *Placenta* **23,** In press.
20. Ohteki, T., Okamoto, S., Nakamura, M., Nemoto, E., and Kumagai, K. (1993) Elevated production of interleukin 6 by hepatic MNC correlates with ICAM-1 expression on the hepatic sinusoidal endothelial cells in autoimmune MRL/lpr mice. *Immunol. Lett.* **36,** 145–152.
21. Yasuda, M., Umemura, S., Osamura, R. Y., Kenjo, T., and Tsutsumi, Y. (1995) Apoptotic cells in the human endometrium and placental villi: Pitfalls in applying the TUNEL method. *Arch. Histol. Cytol.* **58,** 185–190.
22. Lei, H., Furth, E. E., Kalluri, R., Chiou, T., Tilly, K. I., Tilly, J. L., Elkon, K. B., Jeffrey, J. J., and Strauss, J. F., 3rd (1996) A program of cell death and extracellular matrix degradation is activated in the amnion before the onset of labor. *J. Clin. Invest.* **98,** 1971–1978.
23. Hsu, C. D., Meaddough, E., Basherra, H., Harirah, H., and Lu, L. C. (2000) Increased apoptosis in human amnion is associated with labor at term. *Am. J. Reprod. Immunol.* **43,** 255–258.
24. Cirelli, N., Moens, A., Lebrun, P., Gueuning, C., Delogne-Desnoeck, J., Vanbellinghen, A. M., and Meuris, S. (1999) Apoptosis in human term placenta is not increased during labor but can be massively induced in vitro. *Biol. Reprod.* **61,** 458–463.
25. Lynch, D. H., Ramsdell, F., and Alderson, M. R. (1995) Fas and FasL in the homeostatic regulation of immune responses. *Immunol. Today* **16,** 569–574.
26. Uckan, D., Steele, A., Cherry, Wang, B. Y., Chamizo, W., Koutsonikolis, A., Gilbert-Barness, E., and Good, R. A. (1997) Tro-

phoblasts express Fas ligand: A proposed mechanism for immune privilege in placenta and maternal invasion. *Mol. Hum. Reprod.* **3,** 655–662.

27. Kauma, S. W., Huff, T. F., Hayes, N., and Nilkaeo, A. (1999) Placental Fas ligand expression is a mechanism for maternal immune tolerance to the fetus. *J. Clin. Endocrinol. Metab.* **84,** 2188–2194.
28. Hammer, A., Blaschitz, A., Daxbock, C., Walcher, W., and Dohr, G. (1999) Fas and Fas-ligand are expressed in the uteroplacental unit of first-trimester pregnancy. *Am. J. Reprod. Immunol.* **41,** 41–51.
29. Huppertz, B., Frank, H. G., Kingdom, J. C., Reister, F., and Kaufmann, P. (1998) Villous cytotrophoblast regulation of the syncytial apoptotic cascade in the human placenta. *Histochem. Cell Biol.* **110,** 495–508.
30. Bamberger, A. M., Schulte, H. M., Thuneke, I., Erdmann, I., Bamberger, C. M., and Asa, S. L. (1997) Expression of the apoptosis-inducing Fas ligand (FasL) in human first and third trimester placenta and choriocarcinoma cells. *J. Clin. Endocrinol. Metab.* **82,** 3173–3175.
31. Zorzi, W., Thellin, O., Coumans, B., Melot, F., Hennen, G., Lakaye, B., Igout, A., and Heinen, E. (1998) Demonstration of the expression of CD95 ligand transcript and protein in human placenta. *Placenta* **19,** 269–277.
32. Balkundi, D. R., Hanna, N., Hileb, M., Dougherty, J., and Sharma, S. (2000) Labor-associated changes in Fas ligand expression and function in human placenta. *Pediatr. Res.* **47,** 301–308.
33. Kumagai, K., Otsuki, Y., Ito, Y., Shibata, M. A., Abe, H., and Ueki, M. (2001) Apoptosis in the normal human amnion at term, independent of Bcl-2 regulation and onset of labour. *Mol. Hum. Reprod.* **7,** 681–689.
34. Hunt, J. S., Vassmer, D., Ferguson, T. A., and Miller, L. (1997) Fas ligand is positioned in mouse uterus and placenta to prevent trafficking of activated leukocytes between the mother and the conceptus. *J. Immunol.* **158,** 4122–4128.
35. Cohen, G. M. (1997) Caspases: The executioners of apoptosis. *Biochem. J.* **326,** 1–16.
36. Fukuda, H., Tomimatsu, T., Watanabe, N., Mu, J., Kohzuki, M., Endo, M., Fujii, E., Kanzaki, T., and Murata, Y. (2001) Post-ischemic hypothermia blocks caspase-3 activation in the newborn rat brain after hypoxia–ischemia. *Brain Res.* **910,** 187–191.
37. Chen, J., Nagayama, T., Jin, K., Stetler, R. A., Zhu, R. L., Graham, S. H., and Simon, R. P. (1998) Induction of caspase-3-like protease may mediate delayed neuronal death in the hippocampus after transient cerebral ischemia. *J. Neurosci.* **18,** 4914–4928.
38. Tomimatsu, T., Fukuda, H., Endo, M., Watanabe, N., Mu, J., Kohzuki, M., Fujii, E., Kanzaki, T., and Murata, Y. (2001) Effects of hypothermia on neonatal hypoxic-ischemic brain injury in the rat: Phosphorylation of Akt, activation of caspase-3-like protease. *Neurosci. Lett.* **312,** 21–24.
39. Adams, J. M., and Cory, S. (1998) The Bcl-2 protein family: Arbiters of cell survival. *Science* **281,** 1322–1326.
40. Green, D. R., and Reed, J. C. (1998) Mitochondria and apoptosis. *Science* **281,** 1309–1312.
41. Green, D. R. (1998) Apoptotic pathways: The roads to ruin. *Cell* **94,** 695–698.
42. Reed, J. C. (1997) Double identity for proteins of the Bcl-2 family. *Nature* **387,** 773–776.
43. Lea, R. G., al-Sharekh, N., Tulppala, M., and Critchley, H. O. (1997) The immunolocalization of bcl-2 at the maternal–fetal interface in healthy and failing pregnancies. *Hum. Reprod.* **12,** 153–158.
44. Kim, C. J., Choe, Y. J., Yoon, B. H., Kim, C. W., and Chi, J. G. (1995) Patterns of bcl-2 expression in placenta. *Pathol. Res. Pract.* **191,** 1239–1244.
45. Maruo, T., Ishihara, N., Samoto, T., Murakoshi, H., Laoag-Fernandez, J. B., and Matsuo, H. (2001) Regulation of human trophoblast proliferation and apoptosis during pregnancy. *Early Pregnancy* **5,** 28–29.
46. Toki, T., Horiuchi, A., Ichikawa, N., Mori, A., Nikaido, T., and Fujii, S. (1999) Inverse relationship between apoptosis and Bcl-2 expression in syncytiotrophoblast and fibrin-type fibrinoid in early gestation. *Mol. Hum. Reprod.* **5,** 246–251.

ACADEMIC PRESS

Biochemical and Biophysical Research Communications 297 (2002) 1205–1210

BBRC

www.academicpress.com

Histamine H_2 receptor-mediated modulation of local cytokine expression in a mouse experimental tumor model☆

Kohji Takahashi, Satoshi Tanaka, Kazuyuki Furuta, and Atsushi Ichikawa*

Department of Physiological Chemistry, Graduate School of Pharmaceutical Sciences, Kyoto University, Sakyo-ku, Kyoto 606-8501, Japan

Received 12 September 2002

Abstract

Accumulating evidence indicates that histamine is involved in the modulation of cytokine expression patterns. We previously reported that daily treatment with the H_2 receptor antagonist, cimetidine, suppressed tumor growth through alteration of the local cytokine expression pattern. In this study, we used a mouse strain genetically lacking histidine decarboxylase (HDC), to evaluate the role of endogenous histamine synthesis on cytokine expression and tumor development. In the mutant mice, cimetidine had no effect on tumor growth, whereas an H_2 agonist, dimaprit, significantly enhanced tumor growth. When the HDC-deficient mice were implanted with mutant CT-26 cells stably expressing HDC, drastic suppression of tumor growth by cimetidine was observed, which was accompanied by augmentation of mRNA expression of LT-β, TNF-α, and IFN-γ in the tumor tissues. These results suggest that endogenous histamine synthesis in tumor tissues suppresses local tumor immunity via the H_2 receptors, resulting in tumor growth promotion.

Keywords: Histamine; Histamine H_2 receptor; Cimetidine; Tumor immunity; Cytokine; Histidine decarboxylase

Histamine has diverse physiological functions in the digestive [1], neuronal [2], and immune systems [3–5]. In the immune system, the IgE-mediated massive release of histamine from mast cells and basophils in anaphylactic responses has been studied intensively [6], whereas the modulatory functions of histamine on cytokine expression profiles and helper T-cell responses have recently been focused on [7–11]. Tumor progression has also been found to be modulated by histamine [12]. Many clinical trials have demonstrated that histamine H_2 receptor antagonists have the potential to improve survival in some types of cancer [13–15]. Although many in vitro and in vivo studies on the modulatory roles of histamine in tumor development have been reported, it remains controversial as to how histamine promotes the development of some types of tumors [5,16]. Recent findings on the role of histamine in the immune system have shed new light on this field. We recently demonstrated that a daily injection of an H_2 antagonist, cimetidine, suppressed tumor progression in mice having received a syngeneic transplantation of CT-26 cells, a colon adenocarcinoma cell line [17]. In this model, high levels of histamine synthesis by infiltrated leukocytes in the tumor tissues were observed, whereas the intratumoral expression of cytokines, such as LT-β, TNF-α, and IFN-γ, were decreased simultaneously with the tumor development. The expression of these protective cytokines was restored upon daily treatment with cimetidine. This result strongly indicates that endogenously produced histamine suppresses local cytokine expression in tumor tissues, although it remains to be fully clarified whether local histamine synthesis is directly involved in the suppression of cytokine expression, and whether the effect of cimetidine is solely mediated by the blocking of H_2 receptors.

☆ *Abbreviations:* cDNA, complementary DNA; GAPDH, glyceraldehyde-3-phosphate dehydrogenase; HDC, L-histidine decarboxylase; IFN, interferon; IL, interleukin; LT, lymphotoxin; RPA, ribonuclease protection assay; TNF, tumor necrosis factor; TGF, transforming growth factor.

* Corresponding author. Fax: +81-75-753-4557.
E-mail address: aichikaw@pharm.kyoto-u.ac.jp (A. Ichikawa).

0006-291X/02/$ - see front matter © 2002 Elsevier Science (USA). All rights reserved.
PII: S0006-291X(02)02360-4

Histamine synthesis in mammals is regulated by the rate-limiting enzyme, L-histidine decarboxylase (HDC: EC 4.1.1.22). We recently developed a mutant mouse strain expressing HDC lacking the domain responsible for its enzyme activity [18]. This mutant strain is resistant to IgE-dependent cutaneous and systemic anaphylaxis [19,20] and exhibits abnormal granule formations in peritoneal mast cells [18]. In the current study, we investigated the involvement of endogenous histamine synthesis in tumor development using these HDC-deficient mice.

Materials and methods

Animals. Five-week-old male Balb/c mice were obtained from Shimizu Experimental Animal Lab (Kyoto, Japan). HDC-deficient mice, which genetically lack the putative binding site for pyridoxal 5'-phosphate in the HDC protein, were generated as described previously [18]. This strain was back-crossed by eight generations to Balb/c mice and maintained under specific pathogen-free conditions. All the experiments were performed according to the Guideline for Animal Experiments of Kyoto University.

Cell culture. The mouse colon adenocarcinoma cell line, CT-26, was grown in RPMI-1640 medium supplemented with 10% fetal bovine serum in a fully humidified atmosphere of 5% CO_2 at 37 °C.

Histidine decarboxylase assay. Measurement of HDC activity in tumor tissues and cells was performed as previously described [17]. The histamine formed was separated on a cation exchange column, WCX-1 (Shimadzu, Kyoto, Japan) by HPLC and then measured by the *o*-phthalaldehyde method [21].

Preparation of a mutant CT-26 cell line. CT-26 cells were transfected with pcDNA3/HDC7, which contains the full-length HDC cDNA [22], and G-418-resistant clones with high expression levels of HDC mRNA were selected. We confirmed that three individual clones exhibited similar levels of enzyme activity and HDC mRNA expression. The profile of tumor growth in mice injected with each clone was not significantly different. Proliferation of one of the mutant CT-26 cell lines (CT-26/HDC) was evaluated by [^{3}H]thymidine incorporation. Cells were seeded onto 12-well culture plates (2×10^5 cells) and incubated in RPMI-1640 containing 2.5% fetal bovine serum for 6 h followed by the addition of 1 μCi of [^{3}H]thymidine (2 Ci/mmol, NEN, Boston, MA). Cells were harvested after a further 12 h of incubation. Incorporation of [^{3}H]thymidine into the acid insoluble fraction of cells was measured by a liquid scintillation counter [23].

Tumor inoculation and measurement of tumor size. Tumor inoculation was performed as previously described [17]. Briefly, CT-26 cells (1×10^6 cells/0.1 ml) or vehicle was injected intradermally into Balb/c mice or HDC-deficient mice. Cimetidine (0.12 mg/kg/day), dimaprit (0.12 mg/kg/day) or vehicle (saline) was injected subcutaneously and tumor size was measured [17]. Tumor volume (V) was calculated using the values of the largest (a) and the smallest (b) diameters according to the formula: $V = 0.5 \times ab^2$.

Ribonuclease protection assay. Total RNA was extracted from the tumor tissues using ISOGEN (Nippon Gene, Tokyo, Japan) and subjected to the ribonuclease protection assay (RPA). RPA was performed using a multiprobe template set (RiboQuant, Pharmingen, San Diego, CA, mCK-3: LT-β, TNF-α, TNF-β, IL-6, IFN-γ, IFN-β, TGF-β1, and TGF-β2, and two housekeeping genes, L32 and GAPDH) as previously described [17]. The template set was transcribed using a Riboprobe system (Promega, Madison, WI) in the presence of [^{32}P]uridine triphosphate (UTP) (3000 Ci/mmol, NEN, Boston, MA). Total RNA (20 μg) was hybridized with [^{32}P]-labeled antisense RNAs at 56 °C overnight and subjected to ribonuclease treatment. Protected fragments were precipitated and separated onto a 5% acrylamide gel. The gel was dried and analyzed using a Fujix BAS 2000 Bio-Imaging Analyzer.

Results

Effects of cimetidine and dimaprit on CT-26 tumor growth in HDC-deficient mice

We previously demonstrated that daily treatment with an H_2 receptor antagonist, cimetidine, could significantly suppress CT-26 tumor growth in Balb/c mice [17]. In the current study, we performed the syngeneic tumor implantation study using HDC-deficient mice to focus on the role of endogenous histamine synthesis in tumor development. HDC-deficient mice back-crossed by eight generations to the Balb/c strain demonstrated no rejective responses to the implanted CT-26 cells, which were originally established from the Balb/c mice. Daily treatment with cimetidine (0.12 mg/kg) did not change the profile of tumor development nor alter the mRNA expression of any of the cytokines examined in the tumor tissues on Day-14 (Figs. 1A and B). On the other hand, daily treatment with an H_2 agonist, dimaprit (0.12 mg/kg), significantly augmented tumor growth and suppressed the mRNA expression of LT-β, TNF-α, and IFN-γ, but not that of IL-6 and TGF-β (Figs. 1C and D). Similar treatment with dimaprit did not affect tumor growth in the wild type Balb/c mice (data not shown).

Establishment of a mutant CT-26 clone constitutively expressing HDC

We prepared a mutant CT-26 clone (CT-26/HDC), constitutively expressing HDC mRNA, to evaluate the effects of local histamine synthesis on tumor development. This clone exhibited a significant amount of HDC activity, whereas the parental CT-26 cells have no detectable enzyme activity (Table 1). In vitro [^{3}H]thymidine incorporation by CT-26/HDC cells was smaller than that of the parental CT-26 cells under culture conditions in the presence of 2.5% fetal bovine serum (Table 1). The levels of [^{3}H]thymidine incorporation into CT-26/HDC cells were not altered in the presence of cimetidine, pyrilamine (an H_1 antagonist), or thioperamide (an $H_{3/4}$ antagonist) up to a concentration of 100 μM (data not shown), excluding the possibility that histamine produced by CT-26/HDC cells may suppress the cell growth in an autocrine fashion.

Effect of cimetidine on CT-26/HDC tumor growth in HDC-deficient mice

CT-26/HDC cells were successfully implanted into HDC-deficient mice, although the growth rate of the

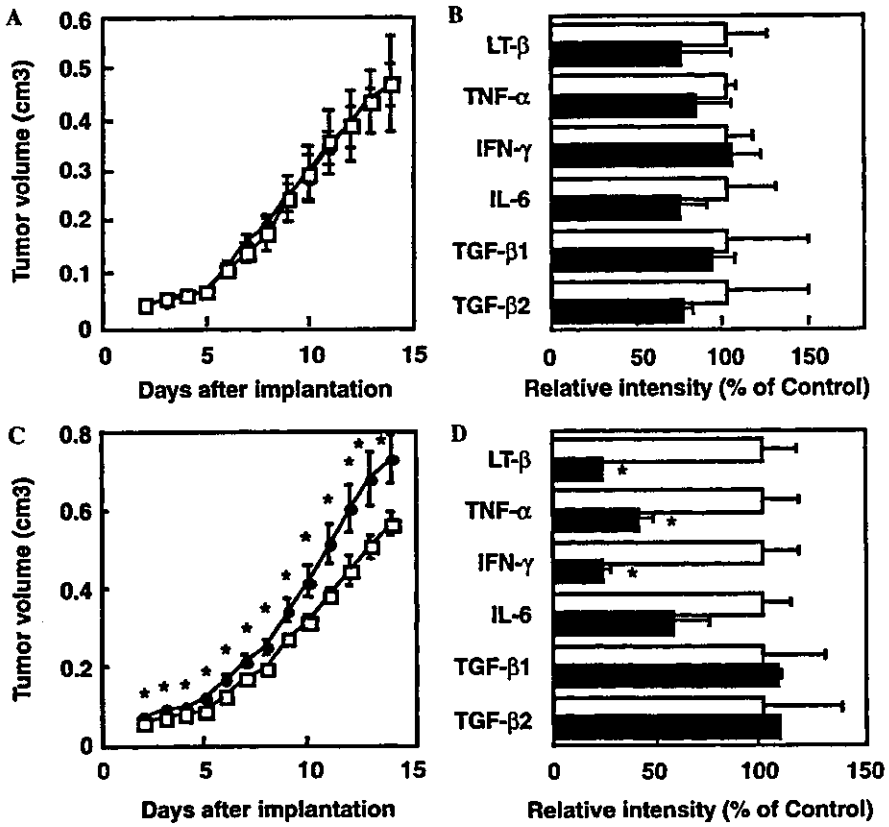

Fig. 1. Promotion of tumor growth and suppression of cytokine expression mediated by histamine H_2 receptors male HDC-deficient mice (5–8 weeks of age) were intradermally injected with CT-26 cells (1×10^6 cells/0.1 ml). The mice were treated with a daily dose of cimetidine (0.12 mg/kg, A and B), or dimaprit (0.12 mg/kg, C and D) for 14 days. (A, C) The volume of each tumor (open boxes, control; closed circles, cimetidine or dimaprit) was measured everyday by the procedure described in the 'Materials and methods.' Values are presented by means ± SEM ($n = 16$). $^*P < 0.05$ is regarded as significant by Student's t test. (B, D) Total RNA (20 μg/lane) extracted from each tumor on Day-14 (open columns, control; closed columns, cimetidine or dimaprit) was subjected to RPA. [^{32}P]-labeled riboprobes protected from ribonuclease digestion were separated and analyzed using a BAS2000 Bio-Imaging Analyzer. The intensity of each protected band was normalized according to that of GAPDH. The relative intensities are presented as means ± SEM ($n = 3$). $^*P < 0.05$ is regarded as significant by Student's t test.

Table 1
Histamine synthesis and proliferation of CT-26/HDC

Cell	HDC activity	[^{3}H]thymidine incorporation
CT-26	<0.005	100 ± 6.19
CT-26/HDC	0.868 ± 0.206	67.8 ± 1.24*

HDC activity and [^{3}H]thymidine incorporation were measured as described in Materials and methods. Results are presented as means ± SEM (HDC activity, pmol/min/mg protein, $n = 5$, [^{3}H]thymidine incorporation, % of incorporation by CT-26 cells, $n = 5$).
$^*P < 0.05$ is regarded as significant by Student's t test.

Table 2
HDC activity in Day-14 tumor tissues

Mouse strain	Balb/c	HDC$^{-/-}$	
Implanted tumor cells	CT-26	CT-26	CT-26/HDC
HDC activity	0.200 ± 0.0650	< 0.005	0.140 ± 0.0200

Balb/c or HDC-deficient mice were intradermally injected with CT-26 or CT-26/HDC cells. Tumor tissues were collected 14 days after the implantation and subjected to the HDC assay as described in the 'Materials and methods.' Specific enzyme activities of HDC are presented as means ± SEM (pmol/min/mg protein, $n = 6$).

CT-26/HDC tumor was smaller than that of the CT-26 tumor. HDC activity in the CT-26/HDC tumor tissues in HDC-deficient mice on Day-14 was comparable to that in the CT-26 tumor tissues in Balb/c mice (Table 2). Daily treatment with cimetidine (0.12 mg/kg) significantly suppressed tumor growth and drastically augmented the mRNA expression of LT-β, TNF-α, and IFN-γ, but not that of IL-6 and TGF-β (Figs. 2A and B). Treatment with pyrilamine or thioperamide did not affect CT-26/HDC tumor growth (data not shown).

Discussion

We demonstrated in this study that local histamine synthesis in tumor tissues has the potential to suppress

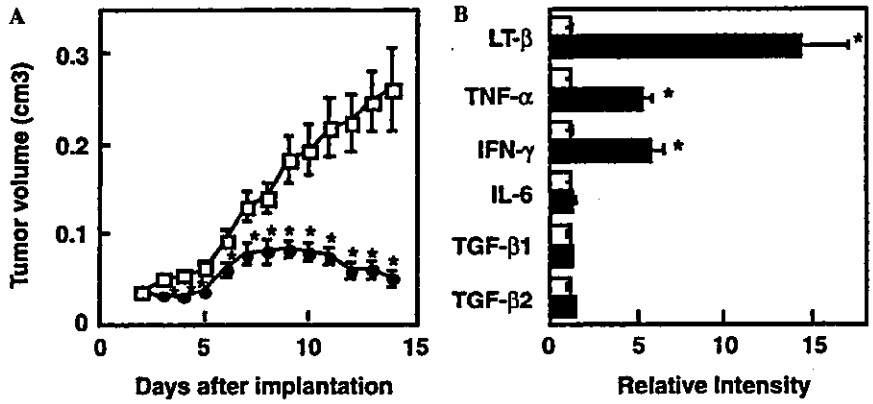

Fig. 2. Inhibitory effect of cimetidine on the growth of CT-26/HDC tumors in HDC-deficient mice. Male HDC-deficient mice (5–8 weeks of age) were intradermally injected with CT-26 cells constitutively expressing HDC (CT-26/HDC, 1×10^6 cells/0.1 ml). The mice were treated daily with cimetidine (0.12 mg/kg) for 14 days. (A) The volume of each tumor (open boxes, control; closed circles, cimetidine) was measured everyday by the procedure described in Materials and methods. Values are presented as means ± SEM ($n = 16$). $^*P < 0.05$ is regarded as significant by Student's t test. (B) Total RNA (20 μg/lane) extracted from each tumor on Day-14 (open columns, control; closed columns, cimetidine) was subjected to RPA. The relative intensities are presented as means ± SEM ($n = 3$). $^*P < 0.05$ is regarded as significant by Student's t test.

tumor development, using HDC-deficient mice. Since neither the HDC-deficient mice [18] nor the colon adenocarcinoma cell line, CT-26, exhibit de novo histamine synthesis (Tables 1 and 2), HDC-deficient mice implanted with CT-26 cells can be treated as a syngeneic tumor model without histamine. Daily treatment with an H_2 antagonist, cimetidine, significantly suppressed CT-26 tumor development in wild type mice [17] whereas not in mutant mice (Fig. 1A), which indicates that the tumor suppressive effect of cimetidine in wild type mice is a result of the inhibition of the H_2-mediated actions of endogenous histamine. Although cimetidine is also known to be a powerful radical scavenger [24], which can affect tumor growth, our observations exclude this possibility. Involvement of the H_2 receptors on tumor growth was also confirmed by the promoting effect of the H_2 agonist, dimaprit, in mutant mice (Fig. 1C). Since histamine is produced by infiltrated leukocytes in the tumor tissue of wild type mice [17], no additive effects of dimaprit may be obtained. Changes in the cytokine expression profiles upon treatment with cimetidine or dimaprit were also consistent with our previous observations [17]. Intratumoral expression of a series of cytokines, such as LT-β, TNF-α, and IFN-γ, which are known to suppress tumor development [25–27], were found to be regulated by H_2 receptors (Figs. 1B and D). Accumulating evidence indicates that the production of several cytokines is regulated by histamine via H_2 receptors. TNF-α production by monocytes and mast cells was found to be directly inhibited by histamine via the H_2 receptors [28,29]. The modulation of IFN-γ production by histamine has been quite controversial. Dohlsten et al. demonstrated that IFN-γ and IL-2 production by purified human T cells is inhibited by histamine via H_2 receptors [30] and these findings have been supported by recent findings that histamine suppresses the production of the Th1-inducing cytokine, IL-12, via H_2 receptors [7,31]. On the other hand, Kohka et al. [32] showed that production of IL-18 and IFN-γ in human peripheral blood mononuclear cells is induced by histamine via H_2 receptors. The former reports are consistent with our results; however, further studies are needed to elucidate this discrepancy.

We prepared a mutant CT-26 cell line (CT-26/HDC), which stably expresses HDC, to investigate the effect of local histamine synthesis in tumor tissues. The degree of CT-26/HDC tumor growth in HDC-deficient mice was smaller than that of the parental CT-26 tumor growth (Figs. 1 and 2), which may be inconsistent with the suppressive effects of histamine on tumor growth via H_2 receptors. However, it is quite difficult to compare the in vivo growth rate of the CT-26/HDC tumor with that of the CT-26 tumor because of the lower in vitro proliferation rate of the mutant cell line (Table 1). Although it remains to be elucidated why the [^{3}H]thymidine incorporation by the mutant cell line was lower than that by the parental CT-26 line, the possibility that histamine suppresses proliferation in an autocrine fashion may be excluded since histamine receptor antagonists did not augment the in vitro growth rate of the CT-26/HDC cells.

In the HDC-deficient mice implanted with CT-26/HDC cells, a much pronounced suppression of tumor growth by cimetidine was observed (Fig. 2). This suppressive effect of cimetidine suggests that local histamine synthesis in tumor tissues is essential for suppression of tumor immunity via H_2 receptors. The drastic augmentation, greater than 5-fold increase, of mRNA expression of antitumoral cytokines, such as LT-β,

TNF-α, and IFN-γ, upon treatment with cimetidine (Fig. 2B) also supports this hypothesis. Jutel et al. [11] recently demonstrated that histamine enhances Th1-type responses via the H_1 receptors, which are the dominant subtype of histamine receptors expressed in Th1 cells, and negatively regulates Th1/Th2-type responses via H_2 receptors. The suppressive effects mediated by H_2 receptors were also reproduced in our system. Furthermore, it is possible that the combination of CT-26/HDC cells and cimetidine treatment augment the Th1-type responses via the H_1 receptors, although no effect of the H_1 receptor antagonist, pyrilamine, on tumor development and cytokine expression could be observed in our system. Modulation of tumor immunity by histamine in our syngenic tumor model may be mainly mediated by H_2 receptors.

In summary, we demonstrated that endogenous local histamine synthesis suppresses the mRNA expression of LT-β, TNF-α, and IFN-γ, via H_2 receptors, resulting in enhancement of tumor growth in the CT-26 syngenic tumor model.

Acknowledgments

We thank Ms. A. Popiel for her help in preparation of the manuscript. This study was supported by grants-in-aid for Scientific Research from the Ministry of Education, Science, Sports, and Culture in Japan.

References

[1] C.F. Code, Histamine and gastric acid secretion: a later look, 1955–1965, Federation Proc. 24 (1965) 1311–1321.
[2] J.C. Schwartz, H. Pollard, T.T. Quach, Histamine as a neurotransmitter in mammalian brain: neurochemical evidence, J. Neurochem. 35 (1980) 26–33.
[3] M.A. Beaven, Histamine, N. Engl. J. Med. 294 (1976) 320–325.
[4] M.V. White, The role of histamine in allergic diseases, J. Allergy Clin. Immunol. 86 (1990) 599–605.
[5] E. Schneider, M. Rolli-Derkinderen, M. Arock, M. Dy, Trends in histamine research: new function during immune responses and hematopoiesis, Trends Immunol. 23 (2002) 255–263.
[6] D.D. Metcalfe, D. Baram, Y.A. Mekori, Mast cells, Physiol. Rev. 77 (1997) 1033–1079.
[7] I.J. Elenkov, E. Webster, D.A. Papanicolaou, T.A. Fleisher, G.P. Chrousos, R.L. Wilder, Histamine potently suppresses human IL-12 and stimulates IL-10 production via H_2 receptors, J. Immunol. 161 (1998) 2586–2593.
[8] J. Sirois, G. Ménard, A.S. Moses, E.Y. Bissonnette, Importance of histamine in the cytokine network in the lung through H_2 and H_3 receptors: stimulation of IL-10 production, J. Immunol. 164 (2000) 2964–2970.
[9] A. Mazzoni, H.A. Young, J.H. Spitzer, A. Visintin, D.M. Segal, Histamine regulates cytokine production in maturing dendritic cells, resulting in altered T cell polarization, J. Clin. Invest. 108 (2001) 1865–1873.
[10] G. Caron, Y. Delneste, E. Roelandts, C. Duez, J. Bonnefoy, J. Pestel, P. Jeannin, Histamine polarizes human dendritic cells into Th2 cell-promoting effector dendritic cells, J. Immunol. 167 (2001) 3682–3686.
[11] M. Jutel, T. Watanabe, S. Klunker, M. Akdis, O.A.R. Thomet, J. Malolepszy, T. Zak-Nejmark, R. Koga, T. Kobayashi, K. Blaser, C.A. Akdis, Histamine regulates T-cell and antibody responses by differential expression of H_1 and H_2 receptors, Nature 413 (2001) 420–424.
[12] J. Bartholeyns, J.R. Fozard, Role of histamine in tumor development, Trends Pharmacol. Sci. 6 (1985) 123–125.
[13] W.J. Adams, D.L. Morris, Short course cimetidine and survival with colorectal cancer, Lancet 344 (1994) 178–1769.
[14] L.B. Svendsen, Cimetidine as an adjuvant treatment in colorectal cancer. A double-blind randomized pilot study, Dis. Colon Rectum. 38 (1995) 514–518.
[15] S. Matsumoto, Cimetidine and survival with colorectal cancer, Lancet 346 (1995) 115.
[16] D.L. Morris, W.J. Adams, Cimetidine and colorectal cancer-old drug, new use?, Nat. Med. 1 (1995) 1243–1244.
[17] K. Takahashi, S. Tanaka, A. Ichikawa, Effect of cimetidine on intratumoral cytokine expression in an experimental tumor, Biochem. Biophys. Res. Commun. 281 (2001) 1113–1119.
[18] H. Ohtsu, S. Tanaka, T. Terui, Y. Hori, Y. Makabe-Kobayashi, G. Pejler, E. Tchougounova, L. Hellman, M. Gertsenstein, N. Hirasawa, E. Sakurai, E. Buzas, P. Kovacs, G. Csaba, A. Kittel, M. Okada, M. Hara, L. Mar, K. Numayama-Tsuruta, S. Ishigaki-Suzuki, K. Ohuchi, A. Ichikawa, A. Falus, T. Watanabe, A. Nagy, Mice lacking histidine decarboxylase exhibit abnormal mast cells, FEBS Lett. 502 (2001) 53–56.
[19] H. Ohtsu, A. Kuramasu, S. Tanaka, T. Terui, N. Hirasawa, M. Hara, Y. Makabe-Kobayashi, N. Yamada, K. Yanai, E. Sakurai, M. Okada, K. Ohuchi, A. Ichikawa, A. Nagy, T. Watanabe, Plasma extravasation induced by dietary supplemented histamine in histamine-free mice, Eur. J. Immunol. 32 (2002) 1698–1708.
[20] Y. Makabe-Kobayashi, Y. Hori, T. Adachi, S. Ishigaki-Suzuki, Y. Kikuchi, Y. Kagaya, K. Shirato, A. Nagy, A. Ujike, T. Takai, T. Watanabe, H. Ohtsu, The control effect of histamine on the body temperature and respiratory function in IgE-dependent systemic anaphylaxis, J. Allergy Clin. Immunol. 110 (2002) 298–303.
[21] P.A. Shore, A. Burkhalter, V.H. Cohn, A method for the fluorometric assay for histamine in tissues, J. Pharmacol. Exp. Ther. 127 (1959) 182–186.
[22] S. Suzuki, S. Tanaka, K. Nemoto, A. Ichikawa, Membrane targeting and binding of the 74 kDa form of mouse L-histidine decarboxylase via its carboxyl-terminal sequence, FEBS Lett. 437 (1998) 44–48.
[23] R. Carlsson, M. Dohlsten, Å. Boketoff, J. Sjöquist, H.O. Sjögren, Staphylococcal protein A (SpA) does not induce production of interferon-γ in human mononuclear blood cells, Cell. Immunol. 86 (1984) 136–144.
[24] K. Uchida, S. Kawakishi, Cimetidine anti-ulcer drug as a powerful hydroxyl radical scavenger, Agric. Biol. Chem. 54 (1990) 2485–2487.
[25] J. Browning, K. Miatkowski, I. Sizing, D. Griffiths, M. Zafari, C.D. Benjamin, W. Meier, F. Mackay, Signaling through the lymphotoxin β receptor induces the death of some adenocarcinoma tumor lines, J. Exp. Med. 183 (1996) 867–878.
[26] B.J. Sugarman, B.B. Aggarwal, P.E. Hass, I.S. Figari, M.A. Palladino, H.M. Shepard, Recombinant human tumor necrosis factor-α: effects on proliferation of normal and transformed cells in vitro, Science 230 (1985) 943–945.
[27] H. Hock, M. Dorsh, U. Kunzendorf, Z. Qin, T. Diamantstein, T. Blankenstein, Mechanism of rejection induced by tumor cell-targeted gene transfer of interleukin 2, interleukin 4, interleukin 7, tumor necrosis factor, or interferon γ, Proc. Natl. Acad. Sci. USA 90 (1993) 2774–2778.

[28] E. Vannier, L.C. Miller, C.A. Dinarello, Histamine suppresses gene expression and synthesis of tumor necrosis factor α via histamine H_2 receptors, J. Exp. Med. 174 (1991) 281–284.
[29] E.Y. Bissonnette, Histamine inhibits tumor necrosis factor-α release by mast cells through H_2 and H_3 receptors, Am. J. Respir. Cell Mol. Biol. 14 (1996) 620–626.
[30] M. Dohlsten, H.O. Sjögren, R. Carlsson, Histamine acts directly on human T cells to inhibit interleukin-2 and interferon-γ production, Cell. Immunol. 109 (1987) 65–74.
[31] T.C.T.M. van der Pour Kraan, A. Snijders, L.C.M. Boeije, E.R. de Groot, A.E. Alewijnse, R. Leurs, L.A. Aarden, Histamine inhibits the production of interleukin-12 through interaction with H_2 receptors, J. Clin. Invest. 102 (1998) 1866–1873.
[32] H. Kohka, M. Nishibori, H. Iwagaki, N. Nakaya, T. Yoshino, K. Kobashi, K. Saeki, N. Tanaka, T. Akagi, Histamine is a potent inducer of IL-18 and IFN-γ in human peripheral blood mononuclear cells, J. Immunol. 164 (2000) 6640–6646.

Expressions of Cyclooxygenase-2 and Prostaglandin E-Receptors in Carcinoma of the Gallbladder: Crucial Role of Arachidonate Metabolism in Tumor Growth and Progression[1]

Toru Asano, Junichi Shoda,[2] Tetsuya Ueda, Toru Kawamoto, Takeshi Todoroki, Manabu Shimonishi, Tadashi Tanabe, Yukihiko Sugimoto, Atsushi Ichikawa, Michihiro Mutoh, Naomi Tanaka, and Masanao Miwa

Departments of Gastroenterology [T. A., J. S., M. M., N. T.] and Gastrointestinal Surgery [T. K., T. T.], Institute of Clinical Medicine, University of Tsukuba, Tsukuba-shi, Ibaraki 305-8575; Department of Pharmaceutical Research, Mitsubishi Kagaku Bio-Clinical Laboratories, Inc., Itabashi-ku, Tokyo 174-8555 [T. U.]; Department of Pharmacology, National Cardiovascular Center Research Institute, Fujishirodai, Suita, Osaka 565-8565 [M. S., T. T.]; Department of Physiological Chemistry, Faculty of Pharmaceutical Sciences, University of Kyoto, Yoshida, Sakyo-ku, Kyoto 606-8501 [Y. S., A. I.]; Cancer Prevention Division, National Cancer Research Institute, Chuo-ku, Tokyo 104-0045 [M. M.]; and Department of Biochemistry and Molecular Oncology, Institute of Basic Medical Science, University of Tsukuba, Tsukuba-shi, Ibaraki 305-8575 Japan [M. M.]

ABSTRACT

An association of gallbladder carcinoma with cholelithiasis suggests that chronic inflammation may modulate tumorigenesis and/or progression of the carcinoma. An enhanced expression of cyclooxygenase-2 (COX-2) is observed frequently in advanced carcinomas of gastrointestinal tracts, which in turn suggests that potentiated arachidonate metabolism may play a crucial role in tumor biology. In the present study, the expression levels of COX-2 and prostaglandin E receptor subtypes were determined in 16 cases of gallbladder carcinomas of different depths of invasion (pT_1 3, pT_2 2, pT_3 4, and pT_4 7) to determine the role of arachidonate metabolism in tumor growth and progression. The mRNA levels of COX-2 were increased significantly in pT_3 and pT_4 carcinomas compared with the levels in pT_1 and pT_2 carcinomas. Immunohistochemistry and *in situ* hybridization revealed the existence of COX-2 mRNA and protein in both the cancerous epithelia and adjacent stroma of pT_1-pT_4 carcinomas. Only in pT_3 and pT_4 carcinomas was intense expression of COX-2 observed in the adjacent stroma. The tissue concentration of PGE_2 was significantly increased in pT_3 and pT_4 carcinomas. The mRNAs of PGE receptor subtypes EP_2, EP_3, and EP_4 were amplified in pT_1-pT_4 gallbladder carcinomas, in which their mRNAs and EP_4 protein were expressed mostly in the cancerous epithelia. Treatment with a specific EP_4 agonist, as well as PGE_2 but not EP_2 and EP_3 agonists, up-regulated the expression of c-fos, an induced growth response gene, and increased colony formation. In advanced gallbladder carcinoma, enhanced expression of COX-2 is observed in the adjacent stroma rather than in the cancerous epithelia, and the stroma is a potent source of PG synthesis. In epithelial-stromal interactions, the increased PGE_2 synthesis in the adjacent stroma and its biological effect via EP_4 on the carcinoma cells may contribute to tumor growth and progression of gallbladder carcinoma.

INTRODUCTION

Gallbladder carcinoma has been associated with a dismal overall prognosis (1–5). The 5-year survival rate after surgery has been reported recently to be between 5 and 13% (1–5). Although the clinical course of gallbladder carcinoma has been thought to depend on the depth of tumor invasion (6–8), tumorigenesis of gallbladder carcinoma, as well as its growth and progression, is complex and not completely understood. An association of gallbladder carcinoma with cholelithiasis (9) or an anomalous arrangement of the pancreaticobiliary duct (10, 11) suggests that long-term inflammation may modulate tumorigenesis and/or progression of the carcinoma. Supporting this notion, *in situ* lesions of dysplasia are found frequently in the epithelia adjacent to gallbladder carcinoma associated with gallstones (12), which in turn suggests the possibility that the histogenesis of epithelial dysplasia may be attributable to a chronic inflammatory stimulus on the gallbladder by gallstones and that some of the precursor lesions may yield carcinoma. In addition, inflammatory changes are often observed in noncancerous epithelia adjacent to advanced carcinoma (12).

Because a number of studies has shown that arachidonate (13) and PGE_2[3] levels (14, 15) are increased in human carci-

Received 9/28/01; revised 1/3/02; accepted 1/28/02.
The costs of publication of this article were defrayed in part by the payment of page charges. This article must therefore be hereby marked *advertisement* in accordance with 18 U.S.C. Section 1734 solely to indicate this fact.
[1] Supported in part by grants-in-aid for Intrahepatic Calculi from the Ministry of Health and Welfare, Japan, grants-in-aid from the Ministry of Education (No. 09670509), and grants-in-aid from University of Tsukuba Research Projects, Japan.
[2] To whom requests for reprints should be addressed, at Department of Gastroenterology, Institute of Clinical Medicine, University of Tsukuba, 1-1-1 Tennodai, Tsukuba-shi, Ibaraki 305-8575, Japan. Phone: (81)-298-53-3124; Fax: (81)-298-53-3124; E-mail: shodaj@md.tsukuba.ac.jp.

[3] The abbreviations used are: PGE_2, prostaglandine E_2; Ab, antibody; COX, cyclooxygenase; G3PDH, glyceraldehyde 3-phosphate dehydrogenase; ISH, *in situ* hybridization; pT, pathological tumor stage; EP, prostaglandin E-receptor; PLA_2, phospholipase A_2; RT-PCR, reverse transcriptase-PCR; $sPLA_2$-IIA, secretory group IIA phospholipase A_2.

noma tissues, interest has been focused on the expression of inflammatory enzymes in the arachidonate cascade, COXs, and PLA_2s in carcinoma of the gallbladder.

A second isoform of COX, COX-2, is induced by mitogens (16), cytokines (16), and growth factors (17), and it produces PG-involved inflammation (18) and cell growth (19). Recent studies (20–23) have shown that COX-2 mRNA expression is markedly elevated in most tissues of human colorectal carcinomas and have suggested a putative role of COX-2 in the tumorigenesis, growth, and progression of carcinomas. Notifying a biological function of COX-2 in carcinoma tissues, overexpression of COX-2 in carcinoma cells is associated with biochemical changes, including activation of membrane metalloproteinase and PG synthesis (24), which in turn yield the phenotypic change of increased invasiveness of the carcinoma cells (24, 25). Besides COX-2, overexpression of $sPLA_2$-IIA has been shown in gastric (26), breast (27), and hepatocellular carcinomas (28). The increased expression of $sPLA_2$-IIA in carcinoma tissues has been shown to correlate with an increased malignant potential of the carcinoma cells (26, 27) and is likely to contribute to tumor development.

Diverse biological activity of PGE_2 (29–31), *i.e.*, physiological, inflammatory, and immunological functions, can be attributed to four specific G protein-coupled receptors, termed EPs. Recent studies have shown that EP mRNAs are distributed throughout the gastrointestinal tracts (32, 33), and the biological effect of PGE_2 in gastrointestinal tissues involves signaling via EP subtypes. The biological effect of COX-2-derived PGE_2 via EPs on carcinoma cells may be involved in phenotypic changes of the carcinoma cells observed in the process of tumor progression, which may modulate the malignant behavior of carcinoma cells.

To elucidate the role of arachidonate metabolism in tumor growth and progression, the expression levels of COX-2 and $sPLA_2$-IIA, as well as EP subtypes, were determined in gallbladder carcinoma tissues of different depths of invasion. Furthermore, in *in vitro* experiments, a growth promotion of gallbladder carcinoma cells in response to treatment with specific EP_2, EP_3, and EP_4 agonists, as well as PGE_2, was studied.

MATERIALS AND METHODS

Patients. Specimens from 16 patients (7 males and 9 females) with gallbladder carcinomas (3 with pT_1, 2 with pT_2, 4 with pT_3, and 7 with pT_4 carcinomas) were included in the present study. The mean age of the patients was 65 years (range, 52–78 years). The patients had been diagnosed as having gallbladder carcinoma and had undergone operations between April 1997 and December 1999 in the University of Tsukuba School of Medicine Hospital. Gallbladder carcinoma was diagnosed on the basis of histological findings and classified according to the tumor node metastasis classification of the American Joint Committee on Cancer (34). In addition, intact gallbladder specimens were obtained at surgery from 10 subjects who had undergone hepatectomy because of metastatic liver carcinoma.

Immunoblot Analysis of COX-2 in Gallbladder Carcinoma. Immunoblot analysis of COX-2 in lysates of the gallbladder and gallbladder carcinoma was performed as described previously (35). The lysate of Mz-ChA-1 cells (36) was used as a positive control. The proteins (50 μg) were transferred to nitrocellulose filters after electrophoresis, and the filters were probed with antihuman COX-2 Ab (IBL18515; Immuno-Biological Laboratories, Gumma, Japan), developed in an enhanced chemiluminescence system (Amersham, Buckinghamshire, United Kingdom), and exposed to Kodak XAR5 film. Quantitation was carried out by video densitometry.

Immunohistochemical Expression of COX-2 and EP in Gallbladder Carcinoma. Immunostaining of COX-2 was performed by the avidin-biotin complex technique using a Vectastain Elite avidin-biotin complex kit (Vector, Burlingame, CA), as described previously (23). Formalin-fixed, paraffin-embedded specimens were serially sectioned at a thickness of 4 μm, placed onto microscopic slides, and then deparaffinized. The slides were immersed for 30 min in 0.3% hydrogen peroxide/methanol to deplete endogenous peroxidase. Then, nonspecific binding sites were blocked with 0.3% normal goat serum for 20 min. The primary Ab raised against COX-2 or the Ab raised against human EP_4 (Cayman Chemical Co., Ann Arbor, MI) was used at a dilution of 1:100, applied to tissue sections, and incubated at room temperature for 30 min. After washing with PBS, biotinylated goat antirabbit IgG (Vector) was applied onto the tissue sections and incubated at room temperature for 30 min. After washing with PBS, a streptavidin peroxidase reagent was applied and incubated at room temperature for 10 min. Finally, the reaction product was visualized using developing color by incubating the slides in a solution of 0.3% hydrogen peroxide, diaminobenzidine tetrahydrochloride, and PBS. A negative control was made using BSA instead of the Ab against COX-2. Counter staining was done with hematoxylin. Specificity was determined by preabsorption of the anti-COX-2 Ab with the COX-2 synthetic polypeptide, which was used as an immunogen (17 amino acids, position 251–267: TVKDTQAE-MIYPPQVPE) for generation of the Ab (37) before staining. Immunostaining with normal rabbit serum and anti-COX-2 Ab absorbed with the synthetic COX-2 polypeptide was completely negative.

Evaluation of the sections was performed by a single pathologist who was blinded to the clinical characteristics and pathological grade of response. The total number of cancerous epithelia and adjacent stroma cells in each section was evaluated. The immunohistochemical expression of COX-2 in gallbladder carcinoma was evaluated in terms of the intensity and positive rate of the immunostaining in the cancerous epithelia or adjacent stroma cells. The intensity was defined by comparing the intensity in smooth muscles or vascular endothelia as internal built-in controls. Fig. 1 shows pictures representing the intensities of immunostaining of COX-2 in gallbladder tissues. The intensity was graded on a scale of 0–2: (*a*) grade 0 (G_0), an intensity in epithelia or adjacent stroma cells being less intense than that in internal controls or the staining being negative; (*b*) grade 1 (G_1), an intensity being similar to that in internal controls (Fig. 1, *A* and *B*); and (*c*) grade 2 (G_2), an intensity being more intense than that in internal controls (Fig. 1*C*). When >5% of the total number of cancerous epithelia or adjacent stroma cells in each section was scored as grade 1 or 2, the section was judged as being positive for COX-2 staining, and then the positive rate (expressed as a percentage) was calculated by counting the epithelia or stroma cells expressing COX-2.

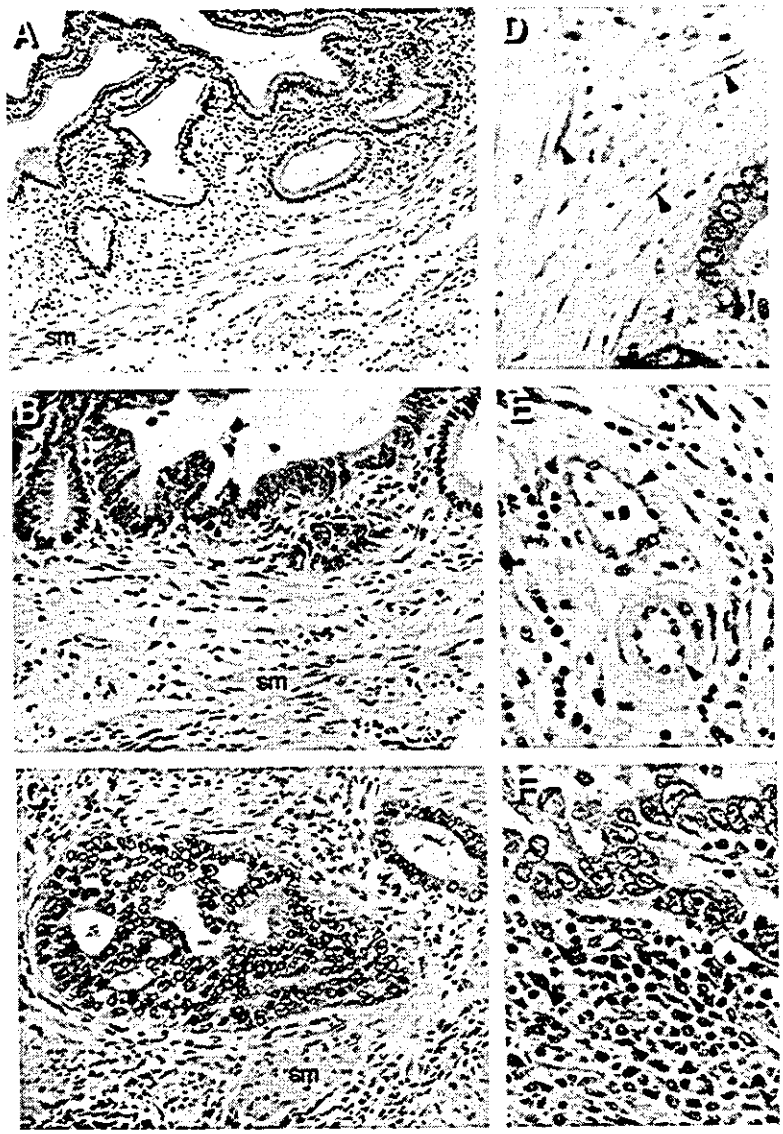

Fig. 1 Grading intensity of immunostaining of COX-2 in gallbladder tissues. *A*, a specimen of intact gallbladder tissue from a patient who underwent cholecystectomy in gastrectomy because of early gastric carcinoma (original magnification: ×33). Weak immunostaining of COX-2 (grade 1 intensity) was observed in the epithelia and smooth muscles (*sm*). *B*, a specimen of gallbladder carcinoma tissue from a case of pT_2 carcinoma (original magnification: ×66). Weak immunostaining of COX-2 (grade 1 intensity) was observed in the cancerous epithelia, whereas the staining was not noted in the stroma. *C*, a specimen of gallbladder carcinoma tissue from a case of pT_4 carcinoma (original magnification: ×66). Intense immunostaining of COX-2 (grade 2 intensity) was observed in both the cancerous epithelia and the stroma adjacent to the epithelia. The COX-2 stainings in the stroma included fibroblasts (*D*; *arrowheads*; original magnification: ×132), vascular endothelial cells (*E*; *arrowheads*; original magnification: ×132), and inflammatory mononuclear cells (*F*; *arrowheads*; original magnification: ×132).

Assay of Tissue Concentration of $sPLA_2$-IIA in Gallbladder Carcinoma. The protein masses of $sPLA_2$-IIA in the tissues of gallbladders and gallbladder carcinomas (ng/mg × protein) were immunoradiometrically assayed as described recently (38). Assay kits were kindly supplied from the Pharmaceuticals Research & Development Division, Shionogi & Co., Ltd. (Osaka, Japan). All assays were performed in triplicate. Protein concentration in the supernatant was measured by the method described by Lowry *et al.* (39).

Assay of Tissue Concentration of PGE_2. Aliquots of tissue homogenates were assayed by a highly specific RIA (Ref. 40; anti-PGE_2 Ab; Amersham, London, United Kingdom) for PGE_2 in duplicate and at two dilutions. The protein contents in the supernatant were measured by the method described by Lowry *et al.* (39). The final results are expressed as pg PGE_2/mg × protein.

RNA Isolation and cDNA Synthesis. Total RNA was isolated from gallbladder carcinoma specimens using Trizol reagent by the modified method described by Chomczynski and Sacchi (41). First-strand cDNAs were synthesized from total RNA with Moloney murine leukemia virus reverse transcriptase by the random primer method.

RT-PCR. Semiquantitative RT-PCR was performed using a DNA Thermal Cycler (model PJ 2000; Applied Biosystems, Inc., Foster City, CA). PCR was subjected to each cycle (G3PDH, 20; COX-1, 30; COX-2, 30; $sPLA_2$-IIA, 35; EP_1, 35; EP_2, 35; EP_3, 35; and EP_4, 35) at 94°C for 1 min, at 55°C for 2 min, and at 72°C for 2 min. Aliquots of the reaction mixture were electrophoresed on a 2% agarose gel. PCR primers were designed from cDNA sequences for human COX-1 (42), COX-2 (43), $sPLA_2$-IIA (44), EP_1 (45), EP_2 (46), EP_3 (47), and EP_4 (48) and then synthesized using an Applied Biosystems DNA

synthesizer (model 392; Applied Biosystems., Inc.) as follows: G3PDH, sense 5′-GAACGGGAAGCTCACTGGCATGGC-3′, antisense 5′-TGAGGTCCACCA CCCTGTTGCTG-3′; COX-1, sense 5′-CTTGACCGCTACCAGTGTGA-3′, antisense 5′-AGA-GGGCAG AATACGAGTGT-3′; COX-2, sense 5′-AAGCCT-TCTCTAACCTCTCC-3′, antisense 5′-TAAGCACAT CGCAT-ACTCTG-3′; $sPLA_2$-IIA, sense 5′-ACCATGAAGACCCTC-CTACTG-3′, antisense 5′-GAAGAG GGGACTCAGCAACG-3′; EP_1, sense 5′-CGCGCTGCCCATCTTCTCCAT-3′, antisense 5′-CCCAGG CCGATGAAGCACCAC-3′; EP_2, sense 5′-GCTGCT-GCTTCTCATTGTCTCG-3′, antisense 5′-TCCGAC AACA-GAGGACTGAACG-3′; EP_3, sense 5′-GGCACGTGGTGCTT-CATC-3′, antisense 5′-GGGTCC AGGATCTGGTTC-3′; and EP_4, sense 5′-ATCTTACTCATTGCCACC-3′, antisense 5′-TC-TATTGCTTTA CTGAGCAC-3′. Plasmid vectors into which each objective coding region of human COX-1 (42), COX-2 (43), $sPLA_2$-IIA (44), EP_1 (45), EP_2 (46), EP_3 (47), and EP_4 (48) had already been inserted were used as positive controls. In each experiment, RT-PCR was done in triplicate. In the semiquantitative assessment, the amounts of fluorescence intensity were measured using a FluorImager (Molecular Dynamics, Sunnyvale, CA). The data were expressed relative to the amount of G3PDH mRNA present in each specimen and then averaged.

Synthesis of cRNA Probes of COX-2 and EP Subtypes. Riboprobes were synthesized from plasmid vectors into which each objective coding region of COX-2, EP_2, EP_3, and EP_4 had already been inserted. Briefly, pBluescript KS containing the coding region of human COX-2 was prepared in the laboratory of Dr. T. Tanabe (National Cardiovascular Center Research Institute, Osaka, Japan). All pBluescript SK containing each coding region of human EP_2, EP_3, and EP_4 were prepared in the laboratory of Prof. A. Ichikawa (Kyoto University, Kyoto, Japan). The inserted coding regions were a 414-bp fragment of human COX-2 (from 7634 to 8047 of D28235, GenBank/EMBL Data Bank; Ref. 43), a 1089-bp fragment of human EP_2 (from 157 to 1245 of U19487, GenBank/EMBL Data Bank; Ref. 46), a 1186-bp fragment of human EP_3 (from 45 to 1230 of ×83857, GenBank/EMBL Data Bank; Ref. 47), and a 1251-bp fragment of human EP_4 (from 362 to 1612 of L28175, GenBank/EMBL Data Bank; Ref. 48). These plasmids were linearized, and antisense RNA probes were transcribed with RNA polymerase in the presence of Cytidine 5′-(α-thio) triphosphate [^{35}S] to a specific activity of 1×10^9 cpm/μg.

ISH of COX-2 and EP Subtypes in Gallbladder Carcinoma. Frozen sections of 8 μm in thickness were cut on a cryostat and thaw mounted onto poly-L-lysine-coated slides. The slides were fixed with 4% formaldehyde in phosphate buffer saline, rinsed in PBS twice, and acetylated with 0.25% acetic anhydride in 0.1 M triethanolamin/0.9% NaCl at room temperature.

ISH was performed as described previously (49). Hybridization was carried out in a buffer containing 50% formamide, 2 × SSC, 10 mM Tris-Cl (pH 7.5), 1 × Denhardt's solution, 10% dextran sulfate, 0.2% SDS, 100 mM DTT, 500 μg/ml sheared single-stranded salmon sperma DNA, and 250 μg/ml yeast tRNA. Riboprobes were added to the hybridization buffer at 7×10^4 cpm/ml. The hybridization solution was applied to the slides, which were then covered with a coverslip and sealed by rubber cement. After incubation at 60°C for 5 h, the slides were immersed in 2 × SCC to remove the coverslips and then washed for 1 h by warming in 2 × SCC and 10 mM β-mercaptoethanol. The sections were then treated with 20 μg/ml RNase A in 0.5 M NaCl, 10 mM Tris-Cl (pH 7.5), and 1 mM EDTA, followed by an additional wash in 0.1 × SSC at 60°C for 1 h. After dehydration, the slides were dipped in NTB-2 emulsion (Eastman Kodak, Rochester, NY) diluted 1:1 with distilled water. After exposure for 4 weeks at 4°C, the dipped slides were developed in COPINAL (FUJIFILM, Tokyo, Japan), diluted 1:2 in distilled water, fixed, and counterstained with H&E.

Cell Line and Culture Conditions. Mz-ChA-1 and Mz-ChA-2, gallbladder adenocarcinoma cell lines (36), were obtained from Dr. A. Knuth (Johaness-Gutenberg University, Mainz, Germany). The cells were maintained in DMEM that contained 10% heat-inactivated FCS (Hyclone Laboratories, Inc., Logan, UT) in a humidified atmosphere with 5% carbon dioxide at 37°C. The biological properties of these two cell lines, *i.e.*, the *in vitro* colony formation, the *in vitro* growth kinetics, and the tumor formation into nude mice, have been described by Knuth *et al.* (36).

Immunoblot analysis of COX-2 in cell protein lysates was performed in the same way as described before. Northern blot analysis was performed using total cellular RNA extracted from the cells. RNA specimens (each 20 μg) were separated on formaldehyde-agarose gels and blotted onto nitrocellulose filters. The blot was hybridized with cDNA probes labeled with [α-^{32}P]dCTP by random primer extension as described previously (50). RT-PCR and ISH of EP mRNAs in the cells were performed in the same ways as described before. PGE_2 production in the cells was determined by measuring PGE_2 concentration in the media from the cells with and without 10 mM arachidonate treatment. The PGE_2 concentration 6 h after the addition of arachidonate was assayed in triplicate by an RIA in the same way as described before (40).

Mz-ChA-2 cells were placed in 24-well tissue culture plates, precultured for 24 h, and then treated with test reagents. In experiments for *c-fos* expression, Mz-ChA-2 cells were grown in complete DMEM with 10% fetal bovine serum for 24 h and then in a medium with 1% FCS for 48 h before being harvested for RNA extraction.

Colony Formation Assay. The colony number of Mz-ChA-2 cells was counted according to the method (51) described previously with minor modifications. Briefly, Mz-ChA-2 cells were plated in a 10-cm cell culture disc at a density of 1000 cells/dish with DMEM containing 10% FCS. A selective EP_2 agonist (ONO-AE1-259; Ref. 52; Ono Pharmaceutical Co., Ltd., Osaka, Japan), EP_3 agonist (ONO-AE-248; Ref. 52), and EP_4 agonist (ONO-AE1-329; Ref. 52) at a concentration of 0.01, 0.1, 1, or 10 μM or PGE_2 (Cayman Chemical Co.) at a concentration of 1 μM was added daily to selected cells, and the medium was replaced every day. The cells were incubated for 14 days, and then the colonies were visualized by staining with 0.2% methylene blue and counted manually. In each experiment, the assay was done in quadruplicate.

Assay of *C-fos* Expression in Gallbladder Carcinoma Cells. To elucidate the mechanism involved in the PGE_2 or EP_4 agonist-induced growth of gallbladder carcinoma cells, the steady-state mRNA level of *c-fos*, one of the earliest induced growth response genes (53), was determined in Mz-ChA-2 cells

with or without a stimulation by semiquantitative RT-PCR. The cells were grown in complete DMEM supplemented with 10% FCS for 24 h and then in serum-free media for 48 h before being harvested for RNA isolation. PGE_2 at a concentration of 1 μM or ONO-AE1-329 at a concentration of 0.01, 0.1, 1, or 10 μM was added to the cells, and the cells were harvested after 30 or 60 min. Isolation of total RNA from the cells and RT-PCR were performed in the same way as described before. PCR was subjected to each cycle (G3PDH, 20; *c-fos*, 25) at 94°C for 1 min, at 55°C for 2 min, and at 72°C for 2 min. PCR primers of *c-fos* were designed from cDNA sequences for human *c-fos* (54) and then synthesized in the same way as described before as follows: *c-fos*, sense 5'-GAATAAGATGGCTGCAGCCAAA-TGCCGCAA-3', antisense 5'-CAGTCAGATCAAGGGAAG CCACAGACATCT-3'. In each experiment, RT-PCR was done in triplicate. The data were expressed relative to the amount of G3PDH mRNA present in each specimen and then averaged.

Statistics. Values are given as means ± SE. Means of two groups were compared with the Mann-Whitney rank sum *U* test (two-tailed test), and multiple comparisons were performed by ANOVA. A two-sided χ^2 test was used for comparison of clinicopathological data between groups. A P of <0.05 was defined as statistically significant.

RESULTS

Immunoblot Analysis of COX-2 in Gallbladder Carcinoma. A limited number of carcinoma tissue specimens (5 specimens from 1 patient with chronic cholecystitis associated with cholelithiasis, 1 patient with pT_2, 2 patients with pT_3, and 1 patient with pT_4 carcinoma) was subjected to immunoblot analysis (Fig. 2). Parallel to the depth of invasion, the carcinoma tissues yielded a prominent band for COX-2; in densitometric analysis, the abundance of the band (expressed as COX-2:β-actin ratio) was significantly higher in 11 specimens of pT_3 and pT_4 carcinomas (0.88 ± 0.08, mean ± SE, $P < 0.01$) than in 5 specimens of pT_1 and pT_2 carcinomas (0.53 ± 0.02) and 10 specimens of normal gallbladders (0.24 ± 0.02).

Immunohistochemical Expression of COX-2 in Gallbladder Carcinoma. In tissue specimens of intact gallbladders, immunostaining of COX-2 was observed in the epithelia and smooth muscles (Fig. 1*A*). The expression levels were weak. However, in tissue specimens of gallbladder carcinomas, intense immunostaining of COX-2 was observed in cancerous epithelia in the specimens of pT_1 and pT_2 carcinomas (data not shown) and in both cancerous epithelia and stroma adjacent to the epithelia in the specimens of pT_3 and pT_4 carcinomas (Fig. 1*C*). The COX-2 stainings in the stroma included fibroblasts (*arrowheads* in Fig. 1*D*), vascular endothelial cells (*arrowheads* in Fig. 1*E*), and inflammatory mononuclear cells (*arrowheads* in Fig. 1*F*). Immunostaining of COX-2 was observed in >80% of cancerous epithelia of pT_1-pT_4 gallbladder carcinomas and normal epithelia of the gallbladders (Table 1). No significant difference in the expression rate of COX-2 was found among the cancerous and normal epithelia. In the epithelia (Table 1), grade 2 intensity of COX-2 expression was observed at a high frequency in pT_1 and pT_2 carcinomas (60%, $P < 0.05$) and pT_3 and pT_4 carcinomas (82%, $P < 0.05$), compared with that in normal epithelia (0%). Grade 1 intensity was observed at a high frequency in normal epithelia (80%). In the stroma adjacent to the cancerous epithelia (Table 1), grade 2 intensity was observed only in the stroma adjacent to pT_3 and pT_4 carcinomas (55%), and the rate of grade 2 intensity in these stroma was significantly higher than that in the stroma adjacent to the normal epithelia (0%, $P < 0.05$). Grade 1 intensity was observed in the stroma of pT_1 and pT_2 carcinomas (20%) and pT_3 and pT_4 carcinomas (27%).

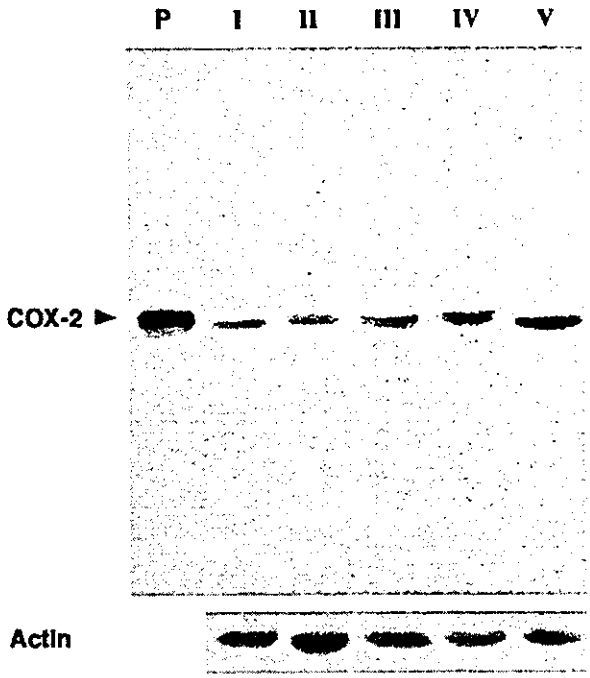

Fig. 2 Immunoblot analysis of COX-2 in Mz-ChA-1 cells and gallbladder carcinoma tissues. *Lane P*, the lysate of Mz-ChA-1 cells; *Lane I*, the lysate of a specimen of normal gallbladder; *Lane II*, the lysate of a specimen from a case of pT1 carcinoma; *Lane III*, the lysate of a specimen from a case of pT2 carcinoma; *Lane IV*, the lysate of a specimen from a case of pT3 carcinoma; *Lane V*, the lysate of a specimen from a case of pT4 carcinoma.

Tissue mRNA Levels of COX-1 and -2, $sPLA_2$, and EP Subtypes in Gallbladder Carcinoma. Fig. 3 shows the PCR-assisted amplifications of COX-1, COX-2, $sPLA_2$-IIA, and EP_{2-4} subtypes in the tissues of normal gallbladders and gallbladder carcinomas of different depths of invasion. The mRNA level of COX-2 was significantly higher in 5 specimens of pT_1 and pT_2 carcinomas (91 ± 17% of G3PDH, mean ± SE, $P < 0.01$) and in 11 specimens of pT_3 and pT_4 gallbladder carcinomas (136 ± 11%, $P < 0.01$), compared with the level in 10 specimens of normal gallbladders (54 ± 5%) as shown in Table 2, whereas the level of COX-1 was not significantly different among the specimens. In terms of the depth of invasion, the mRNA level of COX-2 was significantly higher in the pT_3 and pT_4 carcinomas than in the pT_1 and pT_2 carcinomas ($P < 0.01$). Of the $sPLA_2$ isoforms, the mRNA of $sPLA_2$-IIA was expressed strongly in tissues of gallbladder carcinomas, whereas it was only expressed weakly in tissues of normal gallbladder. Similar to the COX-2 expression pattern, the mRNA level of $sPLA_2$-IIA

Table 1 Immunohistochemical expression of COX-2 in the epithelia and stroma of gallbladder carcinoma of different depths of invasion[a]

	Normal gallbladder (10)				pT_1-pT_2 carcinoma (5)				pT_3-pT_4 carcinoma (11)			
	Positive rate	Intensity			Positive rate	Intensity			Positive rate	Intensity		
		G_0[b]	G_1	G_2		G_0	G_1	G_2		G_0	G_1	G_2
Epithelia	8/10	2	8	0[c]	5/5	0	2	3	11/11	0	2	9[d]
Stroma	0/10[d]	10	0	0	1/5[d]	4	1	0	9/11[c]	2	3	6

[a] Immunostaining of COX-2 was evaluated in terms of the positive rate and intensity (see "Materials and Methods").
[b] G_0, grade 0; G_1, grade 1; G_2, grade 2.
[c] $P < 0.01$, significantly different from other groups.
[d] $P < 0.05$.

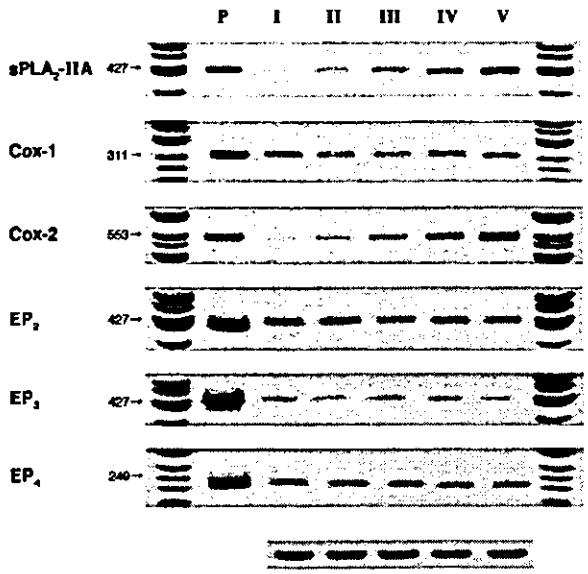

Fig. 3 PCR-assisted amplifications of mRNAs of $sPLA_2$-IIA, COX-1, COX-2, EP_2, EP_3, and EP_4 in gallbladder carcinoma tissues. Plasmid vectors into which each objective coding region of human COX-1 (42), COX-2 (43), $sPLA_2$-IIA (44), EP_2 (46), EP_3 (47), and EP_4 (48) had already been inserted were used as positive controls. *Lane P*, positive controls; *Lane I*, a case of normal gallbladder; *Lane II*, a case of pT_1 carcinoma; *Lane III*, a case of pT_2 carcinoma; *Lane IV*, a case of pT_3 carcinoma; *Lane V*, a case of pT_4 carcinoma. The abundance of G3PDH mRNA was determined as an internal standard. The PCR products were 449 bp in size for $sPLA_2$-IIA, 309 bp for COX-1, 531 bp for COX-2, 392 bp for EP_2, 416 bp for EP_3, 212 bp for EP_4, and 311 bp for G3PDH.

Table 2 Steady-state mRNA levels of $sPLA_2$-IIA, COX-1, and COX-2 and tissue concentrations of $sPLA_2$-IIA and PGE_2 in gallbladder carcinoma of different depths of invasion

	Normal gallbladder (10)	pT_1-pT_2 carcinoma (5)	pT_3-pT_4 carcinoma (11)
Messenger RNA		*% G3PDH*	
$sPLA_2$-IIA	88 ± 10	120 ± 20	200 ± 16[a,b]
COX-1	105 ± 5	107 ± 12	98 ± 12
COX-2	54 ± 5	91 ± 17[c]	136 ± 11[a,d]
Tissue concentration		*pg/mg × protein*	
$sPLA_2$-IIA	0.9 ± 0.1	1.5 ± 0.3	3.9 ± 0.6[a,b]
PGE_2	59.2 ± 7.9	106.2 ± 16.1	257.9 ± 26.1[a,b]

[a] $P < 0.01$, significantly different from normal gallbladder.
[b] $P < 0.01$, significantly different from pT_1-pT_2 carcinoma.
[c] $P < 0.05$.
[d] $P < 0.05$.

was significantly higher in 5 specimens of pT_1 and pT_2 carcinomas (120 ± 20%, $P < 0.01$) and in 11 specimens of pT_3 and pT_4 gallbladder carcinomas (200 ± 16%, $P < 0.01$), compared with the level in 10 specimens of normal gallbladders (88 ± 10%). In terms of the depth of invasion, the mRNA level was significantly higher in the pT_3 and pT_4 carcinomas than in the pT_1 and pT_2 carcinomas ($P < 0.01$).

Of the EP subtypes, the mRNAs of EP_2, EP_3, and EP_4 were amplified in both tissues of normal gallbladders and gallbladder carcinomas (Fig. 3). The mRNA levels of EP_{2-4} subtypes determined by the semiquantitative assessment were not significantly different among normal gallbladders and pT_1-pT_4 carcinomas. In contrast to COX-2 expression, the expression levels of EP_2, EP_3, and EP_4 mRNAs did not differ significantly in terms of the depth of invasion.

ISH of mRNAs of COX-2 and EP Subtypes in Gallbladder Carcinoma Tissues. COX-2 mRNA was expressed widely in the epithelia and focally in the adjacent stroma in the specimens of pT_4 gallbladder carcinoma tissues (Fig. 4, *A* and *B*). The extent and distribution of COX-2 mRNA resembled that of COX-2 protein in individual cases (data not shown). EP_2, EP_3, and EP_4 mRNAs were predominantly expressed in the cancerous epithelia (Fig. 4, *C*, *D*, and *F*), and the extent and distribution of EP_4 mRNA was consistent with that of EP_4 protein (Fig. 4*E*).

Tissue Concentration of $sPLA_2$-IIA in Gallbladder Carcinoma. The tissue concentration of $sPLA_2$-IIA in gallbladder carcinoma was significantly increased in 5 specimens of pT_1 and pT_2 carcinomas (1.5 ± 0.3 ng/mg × protein, mean ± SE, $P < 0.01$) and in 11 specimens of pT_3 and pT_4 gallbladder carcinomas (3.9 ± 0.6, $P < 0.01$), compared with the concentration in 10 specimens of normal gallbladders (0.9 ± 0.1) as shown in Table 2. In terms of the depth of invasion, the concentration was significantly higher in the pT_3 and pT_4 carcinomas than in the pT_1 and pT_2 carcinomas ($P < 0.01$).

Tissue Concentration of PGE_2 in Gallbladder Carcinoma. In association with the increased COX-2 and $sPLA_2$-IIA expression levels, the tissue concentration of PGE_2 was significantly increased in 5 specimens of pT_1 and pT_2 carcinomas (106.2 ± 16.1 pg/mg × protein, mean ± SE, $P < 0.01$) and